UNITED STATES
DEPARTMENT OF THE INTERIOR
GEOLOGICAL SURVEY

TECHNICAL LETTER NUMBER 11

CRUSTAL STRUCTURE FROM SAN FRANCISCO, CALIFORNIA, TO EUREKA, NEVADA, FROM SEISMIC-REFRACTION MEASUREMENTS*

by

Jerry P. Eaton**

DENVER, COLORADO

This page intentionally left blank

UNITED STATES
DEPARTMENT OF THE INTERIOR
GEOLOGICAL SURVEY

Technical Letter
Crustal Studies-11
March 18, 1963

Dr. Charles C. Bates
Chief, VELA UNIFORM Branch
Advanced Research Projects Agency
Department of Defense
Pentagon
Washington 25, D. C.

Dear Dr. Bates:

Transmitted herewith are 10 copies of:

TECHNICAL LETTER NUMBER 11

CRUSTAL STRUCTURE FROM

SAN FRANCISCO, CALIFORNIA, TO EUREKA, NEVADA,

FROM SEISMIC-REFRACTION MEASUREMENTS*

by

Jerry P. Eaton**

We intend to submit this report for publication in a scientific journal.

Sincerely,

L. C. Pakiser

L. C. Pakiser, Chief
Branch of Crustal Studies

* Work performed under ARPA Order No. 193-62.

** U. S. Geological Survey, Denver, Colorado.

This page intentionally left blank

UNITED STATES
DEPARTMENT OF THE INTERIOR
GEOLOGICAL SURVEY

Technical Letter
Crustal Studies-11
March 18, 1963

CRUSTAL STRUCTURE FROM SAN FRANCISCO, CALIFORNIA, TO EUREKA, NEVADA, FROM SEISMIC-REFRACTION MEASUREMENTS*

By

Jerry P. Eaton**

Abstract. Seismic-refraction measurements from chemical explosions near San Francisco, California, and Fallon and Eureka, Nevada, were made along a line extending nearly 700 km inland from San Francisco across the Coast Ranges, Great Valley, Sierra Nevada, and Basin and Range Province. The velocity of P_g in the Basin and Range Province was found to be 6.0 km/sec. Between Fallon and Eureka the velocity of P_n is 7.8 km/sec, and just east of the Sierra Nevada it is about 7.9 km/sec. Two prominent phases closely following the first arrival between 50 and 250 km from the source in the Basin and Range Province were interpreted as reflections from an intermediate layer and from the Mohorovicic discontinuity. The velocity of P in the possible intermediate layer, deduced from the reflected phases because the refracted wave expected from this layer is nowhere a first arrival, seems to be 6.6 km/sec at the top of the layer and probably increases with depth.

* Work performed under ARPA Order No. 193-62.

** U. S. Geological Survey, Denver, Colorado.

In the Coast Range northeast of San Francisco, the velocity of P in the crust, 5.4 to 5.6 km/sec, is substantially smaller than in the Basin and Range Province. When corrected for abnormal delays in the sediments, first arrivals from San Francisco across the Great Valley suggest a P_n velocity of 7.9 km/sec. The low apparent velocity of first arrivals on this profile beyond the valley indicates that the Moho dips downward beneath the Sierra.

From a depth of about 20 km beneath the Coast Ranges and Great Valley, the Moho descends to at least 40 km beneath the high Sierra. East of the Sierra it rises rapidly to about 22 km beneath Carson Sink and then dips downward toward Eureka, where it reaches a depth of 32 km. If the intermediate layer is real, the foregoing depths are increased by 2 to 5 km.

UNITED STATES
DEPARTMENT OF THE INTERIOR
GEOLOGICAL SURVEY

Technical Letter
Crustal Studies-11
March 18, 1963

CRUSTAL STRUCTURE FROM SAN FRANCISCO, CALIFORNIA, TO EUREKA, NEVADA, FROM SEISMIC-REFRACTION MEASUREMENTS*

By

Jerry P. Eaton**

Introduction. Seismograms analyzed in this paper were derived from chemical explosions at three shotpoints: "San Francisco," in the Pacific Ocean about 25 km southwest of the Golden Gate, California; "Fallon," in Soda Lake about 10 km northwest of Fallon, Nevada; and "Eureka," in drill holes near the east edge of Newark Valley about 25 km east of Eureka, Nevada. They were recorded along a line extending inland about 700 km from San Francisco that is nearly perpendicular to the major structural trends of the geologic provinces it traverses: Coast Ranges, Great Valley of California, Sierra Nevada, and Basin and Range. The work was done as a part of the VELA UNIFORM program of the Advanced Research Projects Agency, Department of Defense.

This long line is made up of four seismic profiles: San Francisco to Fallon, Fallon to San Francisco, Fallon to Eureka, and Eureka to Fallon. The distance between shotpoints at San Francisco and Fallon (394 km) was too great for the execution of a reversed profile; so these profiles were treated separately. The shotpoints at Fallon and Eureka were sufficiently close together (276 km) that a limited reversal of the profile was achieved. Although subsurface overlap was small, these lines were treated as a reversed profile.

* Work performed under ARPA Order No. 193-62.
** U. S. Geological Survey, Denver, Colorado.

A fifth (unreversed) profile, along the east side of the Sierra from Fallon to Owens Valley, California, provides additional evidence on the nature of the crust near the Fallon shotpoint. Records from one location in the high Sierra and from four locations along the west flank of the Sierra were included with this profile for comparison with records from the east side of the range.

Shotpoints (stars) and recording locations (dots) are plotted on the location map (Fig. 1), which also shows the relation between the profiles and the major geologic features of the region.

For each of these five profiles, the major phases of the compressional-wave group were studied in terms of traveltime, amplitude, and period. Traveltime proved to be the most useful parameter for analysis, although amplitudes were of great help in correlating waves between records. Periods varied little with phase, charge, or distance.

The long-range refraction equipment which recorded the seismograms used in this study has been described by Warrick and others (1961). An outline of field procedures is presented by Jackson, Stewart, and Pakiser (1963) in this symposium.

Chemical charges ranging in size from 1,000 to 11,000 lbs. were detonated to generate seismic waves for the profiles studied. These waves were recorded by 10 refraction units spaced at intervals along a profile, as described by Jackson, Stewart, and Pakiser (1963).

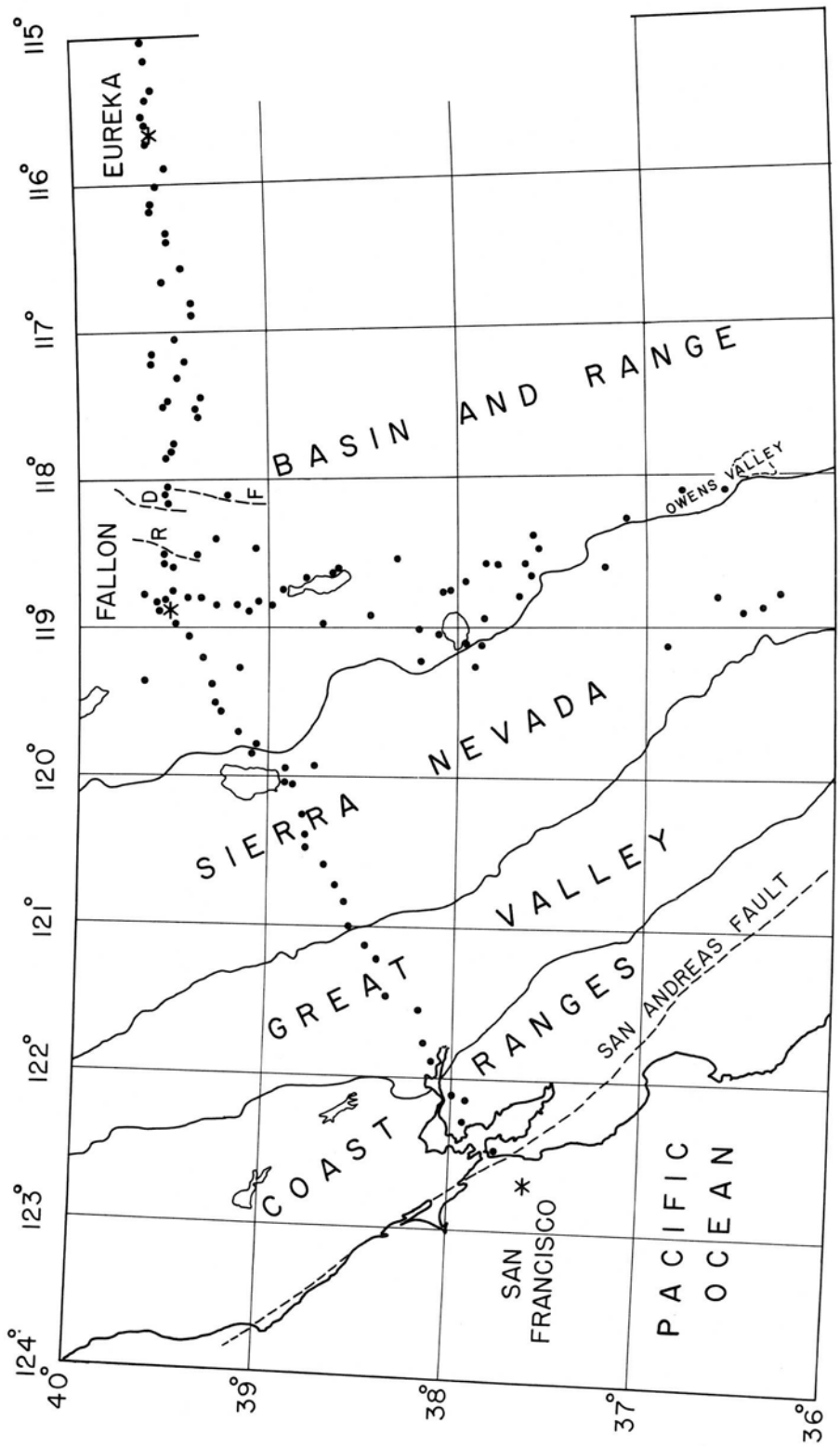

Figure 1.-- Location map showing relationship of profiles to the geologic provinces they cross. Shotpoints are marked by a star; receiver locations by a dot. Near Fallon, R, D, and F mark the 1954 breaks along the Rainbow Mountain, Dixie Valley, and Fairview faults which were associated with the Fallon-Stillwater and Dixie Valley-Fairview Peak earthquakes of that year.

Information from the seismograms. The most crucial step in reading the seismogram is the identification of significant wave arrivals. "First breaks" are commonly distinct to ranges of 100 to 150 km if background noise is not unusually high. At larger distances or in the presence of high noise, identification is far more difficult. With a single trace, one must rely on a change in amplitude or character (period and general wave structure) to identify the signal. With several seismometers in a linear array, coherence of a suspected signal from seismometer to seismometer and its phase velocity across the spread are additional powerful criteria for distinguishing signal from noise. To identify secondary arrivals one must depend heavily on these criteria, for late-arriving energy from earlier waves keeps the seismometers in constant agitation.

In the analysis of seismograms on which this paper is based, an attempt was made to read all of the distinct phases of the P group: the earliest arrivals plus later arrivals which were strongly coherent across the spread. Not all of these could be correlated from spread to spread, however. Arrival times of each phase at the seismometers nearest and most distant from the shotpoint were measured. Beginnings of phases, the first portion of a wavelet or group of wavelets which could be followed across the spread, not the most prominent "leg" of the phase, were timed. For the period of an arrival, the average time interval between the two most prominent peaks or troughs was adopted. The amplitude of the phase was taken

to be the average of the amplitudes recorded on the vertical seismometers of the largest peak-to-trough swing in the first few half cycles of the arrival, usually the part of the arrival which showed the most distinct "character." Seismograms illustrating the appearance of good records at two shot-to-recorder distances are reproduced in Figure 2. Both records were traced from the low level (-15 db) oscillograph monitors: in each case the high level (0 db) monitor showed clear first breaks, but amplitudes of later phases were too large for tracing. Phase identifications are based on interpretations of the traveltime curves.

Calibration signals shown at the right were recorded immediately after the shot and with the same filter and gain settings as were used for the seismic signal. With the filters used (37 cps, 36 db/octave high cuts for vertical channels 1 thru 6 and 18 cps, 36 db/octave high cuts for horizontal channels 7 and 8) no difference is observed in the amplitude response of the system to 3 cps and 10 cps calibration signals of the same rms voltage. These frequencies span almost the entire range of those recorded on seismograms of this study; so the voltage response of the seismic-recording system is essentially independent of frequency over the range of interest.

The derivation of an equation for reducing trace amplitudes to ground amplitudes can be carried out conveniently in two steps: (1) calculate the voltage produced across the recorder input terminals by a simple harmonic ground motion of given amplitude and frequency,

and (2) determine the input voltage corresponding to the recorded signal amplitude.

Calibration data supplied by the manufacturer (Hall-Sears) for 50 HS-10 seismometers can be summarized as follows:

	Symbol	Average	Variation
Natural frequency	F	2.04 cps	+7% to -7%
Suspended mass	M	745 gm	+4% to -2%
Coil resistance	r	389 ohms	+8% to -2%
Residual damping	β_o	0.22 (fraction of critical)	+15% to -15%
Electrodynamic constant	G	1.12 volts/cm/sec	+10% to -10%
Electrodynamic damping constant	Γ	645	+21% to -20%

From 2 cps to 100 cps the recorder input impedance, Z, was found to be approximately 1550 ohms (essentially resistive at frequencies of interest). Measured resistances, L, of the seismometer cables were: 60 ohms for channels 3, 4, 7, 8; 180 ohms for channels 2 and 5; 300 ohms for channels 1 and 6.

For the average seismometer on a cable of intermediate length (2 or 5), the total damping $\left[\beta = \beta_o + \Gamma/(r+L+Z)\right]$ is 0.52, 52% of critical.

If the seismometer is subjected to a simple harmonic motion of frequency f and amplitude A,

(1) $$\mathfrak{z} = A \sin 2\pi f t$$

where $\mathfrak{z}$ is the component of ground motion to which the seismometer responds and t is time, then the voltage across the recorder input is

(2) $$E_Z(t) = \frac{2\pi A f^3 G Z}{r + L + Z} \cos\left(2\pi f t - \tan^{-1}\frac{2\beta f F}{F^2 - f^2}\right) \Big/ \left[\left(F^2 - f^2\right)^2 + 4\beta^2 f^2 F^2\right]^{1/2}$$

Let S be the peak-to-trough amplitude, in millimeters, of an event on the seismogram for which we wish to calculate the ground displacement A (Fig. 2). Let C be the peak-to-trough amplitude, in millimeters, on the same seismogram of the calibration signal, for which the metered calibration voltage was $V_{\mu v\,(rms)}$. Then the peak input voltage required to produce the signal S is

(3) $$E_Z = \sqrt{2}\,\frac{S}{C}\,V_{\mu v}$$

Combining equations 2 and 3 and evaluating the result for an average seismometer on a cable of intermediate length,

(4) $$A_{M\mu} = \frac{2.75}{f}\,\frac{S}{C}\,V\left[\left(\frac{4.16}{f^2} - 1\right)^2 + \frac{4.50}{f^2}\right]^{1/2}$$

For frequencies between 2 and 10 cps,

(5) $$A_{M\mu} = \frac{2.6}{f}\,\frac{S}{C}\,V$$ approximately.

The amplitude is in millimicrons if V is expressed in microvolts (rms) and f is in cycles per second.

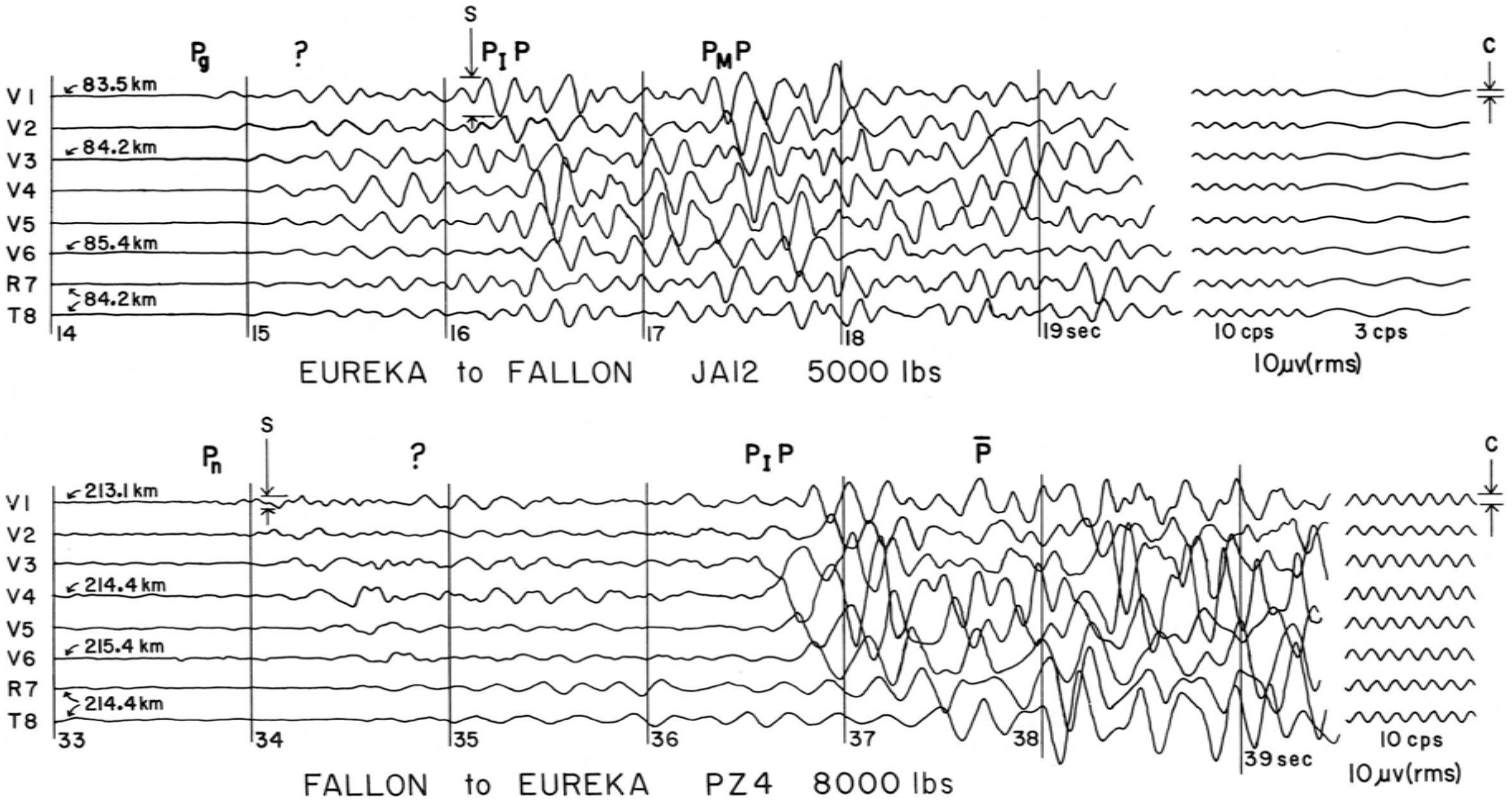

Figure 2.-- Seismograms from the profiles between Fallon and Eureka. The vertical lines indicate seconds past shot time. Individual traces are identified by the component of ground motion measured; vertical (V), radial (R), and transverse (T), as well as by the recording channel, 1-8. Distances from the shot to the nearest receiver, V1, and the farthest receiver, V6, as well as to the three-component "plant" are indicated. Calibration signals recorded with the same instrument adjustments used with the seismic signals are shown on the right. S and C are representative signal and calibration amplitudes from which ground motion amplitudes are calculated. "Up" on the trace corresponds to ground motion up, away from the shot, and clockwise about the shot (viewed from above) for V, R, and T, respectively.

Equation (5) was used to reduce all measured seismogram amplitudes to ground motion. Deviations in individual seismometer responses from the average are no larger than the natural variation in amplitude of a given phase from one end of the spread to the other; so no large error is introduced by using average seismometer characteristics in evaluating average recorded amplitudes.

P in the sialic crust of the Basin and Range Province. Short-range refraction measurements at nine shotpoints in the Basin and Range Province reveal a wide variation in the thickness and velocity of the near-surface rocks which overlie the crystalline crust, with a velocity near 6 km/sec. This variation is responsible for the difference in the intercept of P_g from profile to profile and for the scatter of P_g traveltimes from point to point along a given profile. Velocities in the near-surface rocks fall into two groups, one with an average near 1.9 km/sec and the other with an average near 3.5 km/sec. Rocks of the first group are primarily accumulations of clastic deposits of Cenozoic age in the basins; and those of the second group seem chiefly to be pre-Tertiary sedimentary rocks.

Because the low-velocity near-surface rocks form only an irregular, discontinuous blanket over the crystalline crust, it is the wave refracted through the latter, P_g, that must serve as the seismic datum.

On profiles shot from Fallon and Eureka, P_g emerged as the first arrival within a few kilometers of the shotpoint. It continued as the first arrival to the point at which P_n, the wave refracted along the top of the mantle, emerged ahead of it at distances between 130 and 170 km. First arrivals from Fallon and Eureka were plotted (with a reduced time scale, $T - \Delta/6$ vs Δ) from the shotpoint to the P_n crossover (Fig. 3). The line segments representing wave arrivals connect the time of the phase at the nearest and farthest readable trace on each spread. Along all profiles the velocity of P_g is near 6.0 km/sec. Along each profile, arrival times are scattered through a range of more than half a second about the average line drawn through the arrivals. The maximum ranges in arrival times of P_g about a 6.0 km/sec reference line, over an arbitrary distance interval not larger than 25 km, along individual profiles are: Fallon S, 0.6 sec between 39 and 45 km; Fallon W, 0.6 sec between 83 and 96 km (excluding P_g arrivals in the Sierra); Fallon E, 0.7 sec between 66 and 89 km; Eureka W, 0.6 sec between 56 and 64 km; and Eureka E, 0.5 sec between 21 and 46 km.

The cause of these large variations in arrival times seems clear, for they occur where the profiles cross from the flat alluviated basins onto the ranges between them. Along the profiles reported here, the delay in P_g as it emerges through accumulations of low-velocity deposits in the basins is the chief cause of the observed scatter in P_g arrival times. Similar delays are encountered when the shotpoint is underlain by thick sediments as at Soda Lake in Carson Sink (Fallon shotpoint).

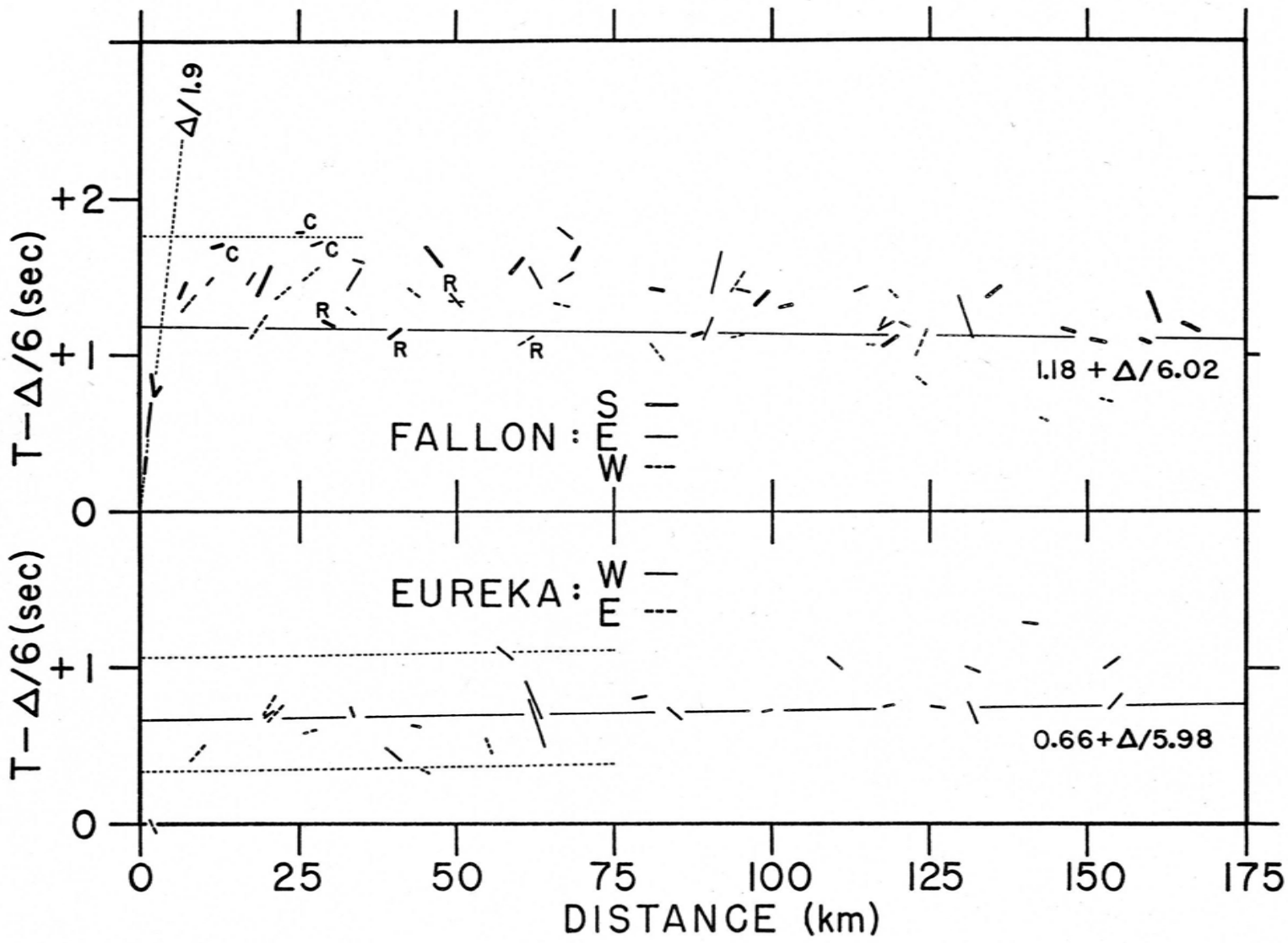
Δ/1.9
+2
+1
0
T−Δ/6 (sec)
C
C
C
R
R
R
R
1.18 + Δ/6.02
FALLON : S
E
W
EUREKA : W
E
0.66+Δ/5.98
0
25
50
75
100
125
150
175
DISTANCE (km)

Figure 3.

Such delays are revealed not by scatter in P_g traveltimes along a given profile but by variations in the P_g intercept from profile to profile.

Because near-surface rocks vary so drastically from point to point along the Basin and Range profiles, it is helpful to formalize the treatment of shotpoint and receiver P_g delays. Let δT_i be the delay of P_g in the surface rocks beneath the receiver R_i, at a distance Δ_i from the shotpoint, and let δT_s be the analogous delay of P_g in the surface rocks beneath the shotpoint. The traveltime of P_g to R_i is $T_i = \frac{\Delta i}{V_g} + \delta T_s + \delta T_i$, where V_g is the velocity of P in the crystalline crust. If δT_i does not vary systematically along the profile and if records from many locations are available, a traveltime line drawn to minimize the sum of the absolute values of the P_g residuals has an intercept $T_o = \delta T_s + \sum_{i=1}^{n} \delta T_i / n$ and a slope $1/V_g$, approximately. If δT_i does vary systematically along the profile, the traveltime graph must be interpreted cautiously.

First arrivals out to 170 km along the profile from Fallon to Owens Valley (Fig. 3) vary systematically with distance. Arrivals very near the shotpoint, in Carson Sink, determine a near-surface velocity of about 1.9 km/sec. Arrivals 12 km from the shotpoint, referred to a velocity of 6.0 km/sec, indicate a P_g intercept ($T_i - \Delta_i/6 = \delta T_s + \delta T_i$) of 1.7 seconds. The next spread, recorded nearer the south edge of Carson Sink, indicates a somewhat smaller P_g intercept. Spreads at 30 km and 40 km, both recorded on the range just south of the Sink, suggest an intercept smaller than 1.2 seconds. The next three

spreads, recorded in basins farther south, indicate an intercept of 1.6 to 1.7 seconds. Beyond 75 km there was greater latitude in the choice of recording locations, and sediment-filled basins were avoided because of the high background noise levels. P_g arrivals at these spreads, still referred to velocity of 6.0 km/sec, suggest intercepts between 1.1 and 1.4 seconds.

If a P_g traveltime line is drawn through these arrivals without regard to the geologic environments of the spreads, the preponderance of "basin" spreads near Fallon leads to an overestimate of both the intercept and velocity of P_g. To minimize this difficulty, wave arrivals recorded at spreads on ranges near Fallon were identified (R) (Fig. 3). The P_g line was then drawn through these and more distant "range" arrivals along the Fallon S profile: its equation is $T = 1.18 + \Delta/6.02$. This line also fits the range arrivals on the Fallon E and Fallon W profiles sufficiently well that it will be adopted as the P_g traveltime curve for all profiles from Fallon.

$P_g(?)$ arrivals beyond 125 km on the Fallon W profile appear to lead this line by a significant amount.

On the assumption that the depth of fill in Carson Sink varies little over the central part of the sink, δT_s can be estimated. For arrivals at stations near the shotpoint in the central part of the sink (C on Fig. 3) $\delta T_i = \delta T_s$, approximately; and $\delta T_i + \delta T_s = 1.76$ second, the intercept of the dotted line drawn parallel to P_g and through the Carson Sink arrivals. Thus, the Fallon shotpoint P_g delay is 0.88 second. From this result and the 1.18 second P_g intercept, it follows that the average P_g delay beneath a range spread is 0.30 second.

From the Eureka shotpoint P_g was recorded to a distance of 155 km toward the west and 55 km toward the east. As amplitudes were generally small, late arrivals at distances beyond 100 km are not reliable as first breaks; and they were given little weight in the determination of the traveltime line. Although the most striking feature of this traveltime curve is the sequence of three spreads from 56 to 64 km where the profile crosses a buried fault between Antelope Valley and the Monitor Range, with a change of 0.64 seconds in P_g delay, there appears to be no systematic variation in P_g delay from one end of the profile to the other. The P_g line through the Eureka data drawn to favor the superior westward profile is $T = 0.66 + \Delta/5.98$. Lines parallel to this one, drawn to bracket early and late arrivals from 0 to 75 km, have intercepts of 0.33 and 1.06 seconds, respectively. The lower limit sets the maximum value of δT_s at 0.33 second and the minimum value of the average range P_g delay at 0.33 second.

The difference in P_g velocity obtained from the Fallon and Eureka profiles is only 0.04 km/sec. Variations in P_g delays along all profiles and the difference in P_g intercepts at Fallon and Eureka are substantial. Such large variations in P_g delays force us to consider techniques for evaluating delays suffered by waves emerging from deeper horizons when they traverse the near-surface rocks.

Traveltime corrections. Corrections to observed traveltimes for known variations in near-surface rocks and ground surface elevation are essential in the analysis of a profile such as that from San Francisco

to Fallon, which begins at sea level on the continental margin, crosses the Coast Ranges and the deep, sediment-filled Great Valley, and ascends the west slope of the Sierra Nevada to receiver elevations greater than 7000 feet. Corrections applied in this paper were those calculated to yield traveltimes which would have been observed if the earth were flat and if the crystalline crust extended to the surface at each shotpoint and receiver.

No correction to P_g is required for a simple change in ground surface elevation along the profile, because the horizontal distances traveled by P_g are very large compared to changes in surface elevation. To correct the traveltime of a wave emerging from beneath the upper surface of the crystalline crust and traveling with an apparent velocity, $\bar{V}$, greater than V_g, to a common (usually shotpoint) datum, subtract from it $\delta T = \delta h \sqrt{\bar{V}^2 - V_g^2} / \bar{V} V_g$, where δh is the elevation of the receiver minus that of the shotpoint. For V_g = 6.0 km/sec and $\bar{V}$ = 8.0 km/sec, δT (sec) = 0.11 δh (km). This correction "subtracts" a slab of crust of appropriate thickness to adjust the receiver elevation to that of the shotpoint.

To correct for near-surface low-velocity materials, they were "replaced" by rock with velocity V_g. Except for particular receivers at crucial locations such as those in the Great Valley, the near-surface corrections were not applied to individual receivers. They were applied to shotpoints and to the "average receiver" on the basis of observed P_g intercepts and delays.

On the basis of results from the shotpoint surveys, which indicated prevalent near-surface velocities of 1.9 km/sec and 3.5 km/sec, the near-surface rocks might be represented by $d_{1.9}$ km of material with a velocity of 1.9 km/sec overlying $d_{3.5}$ km of material with a velocity of 3.5 km/sec which in turn rests on crustal rocks with a velocity of 6.0 km/sec. If all boundaries are flat, near-surface delays of P_g and of waves with apparent velocities of 7.0 km/sec and 8.0 km/sec would be: $P_g, \delta T$ (sec) $= 0.50\ d_{1.9} + 0.23\ d_{3.5}$; $\bar{V} = 7.0, \delta T$ (sec) $= 0.42\ d_{1.9} + 0.16\ d_{3.5}$; and $\bar{V} = 8.0, \delta T$ (sec) $= 0.40\ d_{1.9} + 0.15\ d_{3.5}$.

A realistic estimate of the effect of thick sedimentary deposits on traveltimes of seismic waves cannot neglect the increase in velocity with depth in such materials, however. Hafner (1940) used the linear velocity-depth relationship $V = V_o + AZ$, where V is the velocity at depth Z and V_o is the near-surface velocity, in a discussion of seismic velocities in the Tertiary basins of California. For the part of the Great Valley crossed by the San Francisco to Eureka profile, he reported that an average value for A is about 0.55. Velocity logs from several wells along this profile indicate a one-way traveltime from 0 to 6000 feet, along a vertical path, of about 0.79 second. With A = 0.55, this result requires that $V_o = 1.85$ km/sec. Because nearly the same velocity (1.9 km/sec) was found for the near-surface materials in sediment-filled basins in the Basin and Range province by the shotpoint surveys, the law $V = 1.9 + 0.55\ Z$ was used to calculate near-surface delays in both regions.

For a flat-bottomed basin of depth h and velocity 1.9 + 0.55 Z overlying a crust with velocity 6.0 km/sec, near-surface delays of P_g (velocity 6.0 km/sec) and of waves with apparent velocities of 7.0 km/sec and 8.0 km/sec are presented as functions of h in Figure 4. Along a profile confined to the basin, P_g emerges ahead of the direct wave through the sediments at a distance Δx (Fig. 4) and its traveltime line has an intercept equal to twice the P_g delay. The curves in Figure 4 were terminated at h = 7.46 km, at which depth the velocity nominally reaches 6.0 km/sec. The linear velocity law fails at great depths, and the velocity in the sediments probably approaches that in the crust rather gradually. Such considerations do not detract seriously from the usefulness of the law in estimating traveltime delays in the sediments because the shallow part of the basin in which the law holds fairly well is responsible for most of the delay.

Possible differences in the overall interpretation of a profile that might result from different near-surface velocity models were evaluated for a specific case. The average range P_g delay on the Fallon to Owens Valley profile is 0.3 seconds. The thickness of the near-surface "layer" and, more important, the corresponding near-surface delays of waves with apparent velocities of 8.0 km/sec (P_n) and 7.0 km/sec (P*) were calculated for three models: (1) a single layer with velocity 1.9 km/sec, (2) a single layer with velocity 3.5 km/sec, and (3) a "basin" with velocity 1.9 + 0.55 Z. In all three models V_g was assumed to be 6.0 km/sec.

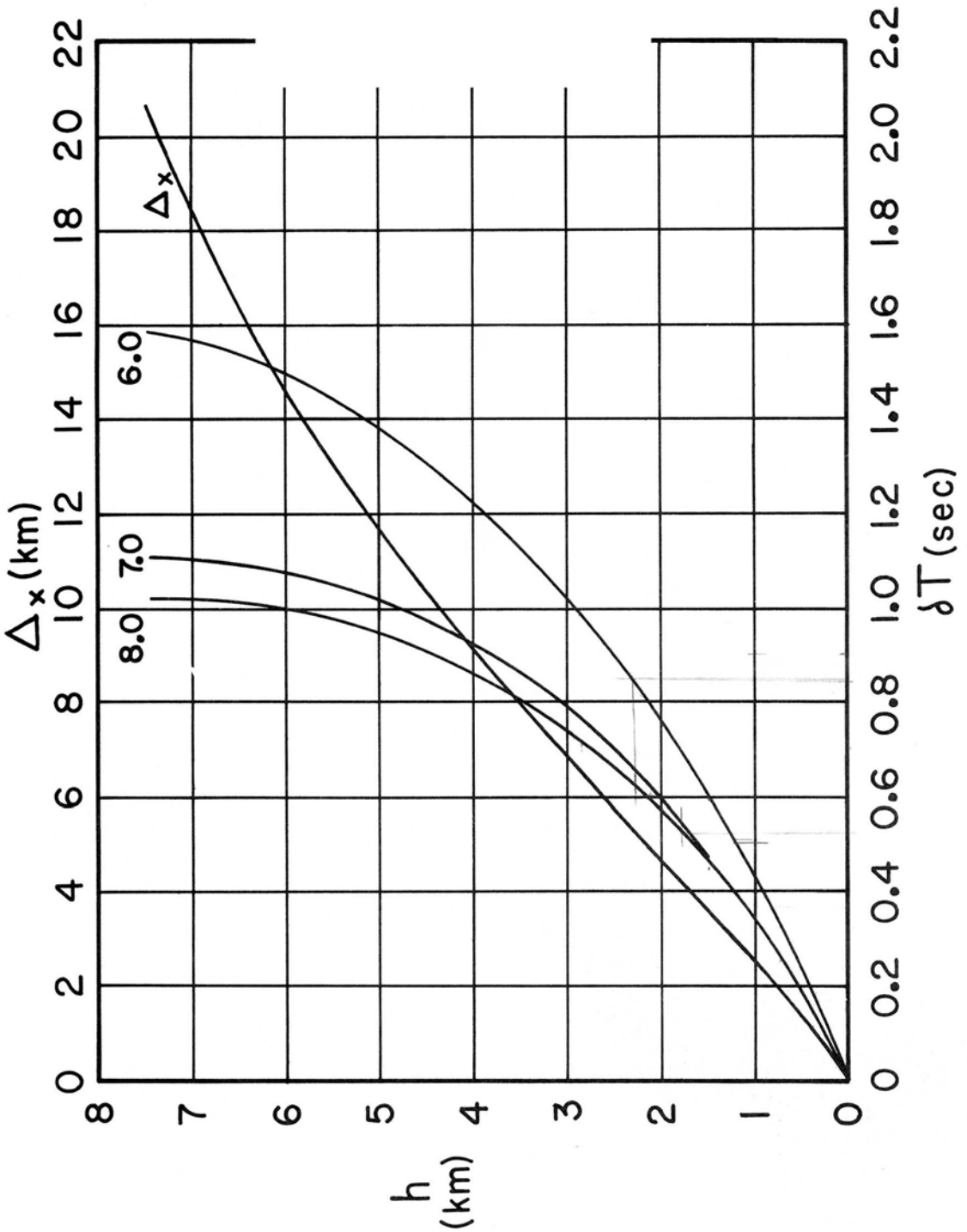

Figure 4.-- Traveltime delays in sediments. Near-surface delays, δT, for waves with apparent velocities of 6.0 km/sec (P_g), 7.0 km/sec (P*), and 8.0 km/sec (P_n) emerging through a sedimentary basin of depth h and velocity 1.9 + 0.55 Z km/sec overlying a crust of velocity 6.0 km/sec are plotted as a function of h. Z is depth in km. Δ_x, the distance at which P_g emerges ahead of the wave refracted through the sediments, is also plotted as a function of h. In the basin, the P_g traveltime line intercept is twice the P_g delay.

Model	P_g delay (sec)	h (km)	P_n delay (sec)	P* delay (sec)
1	0.30	0.60	0.24	0.25
2	0.30	1.3	0.19	0.21
3	0.30	0.65	0.23	0.23

Although the different models lead to different estimates of the thickness of the low velocity rocks above the crust, they yield rather similar corrections to arrival times of waves from deeper boundaries.

For the sake of uniformity, the linear velocity law was used for all near-surface corrections applied in the treatment of the data.

Traveltime curves. Near the point where the P_n and P_g lines cross, several waves of interest arrive within an interval of only one second. Reduced traveltime plots on which $T - \Delta/V$ is plotted vs Δ, where T is the traveltime of a wave to distance Δ and V is a convenient velocity, are capable of much higher time resolution than the familiar time-distance graphs. To illustrate the appearance of a reduced traveltime curve and to anticipate and clarify some results from the Basin and Range profiles, a reduced traveltime diagram for a particular structure is depicted in Figure 5. For a two layer crust consisting of a 6.0 km/sec "granitic" layer 18 km thick lying on a 6.7 km/sec "intermediate" layer 12 km thick above a 7.8 km/sec mantle, traveltime curves were drawn for P_g, P*, and P_n as well as for P_IP, the wave reflected from the top of the intermediate layer, and for P_MP, the wave reflected from the top of the mantle. On the reduced traveltime diagram $T - \Delta/6$ was plotted vs Δ.

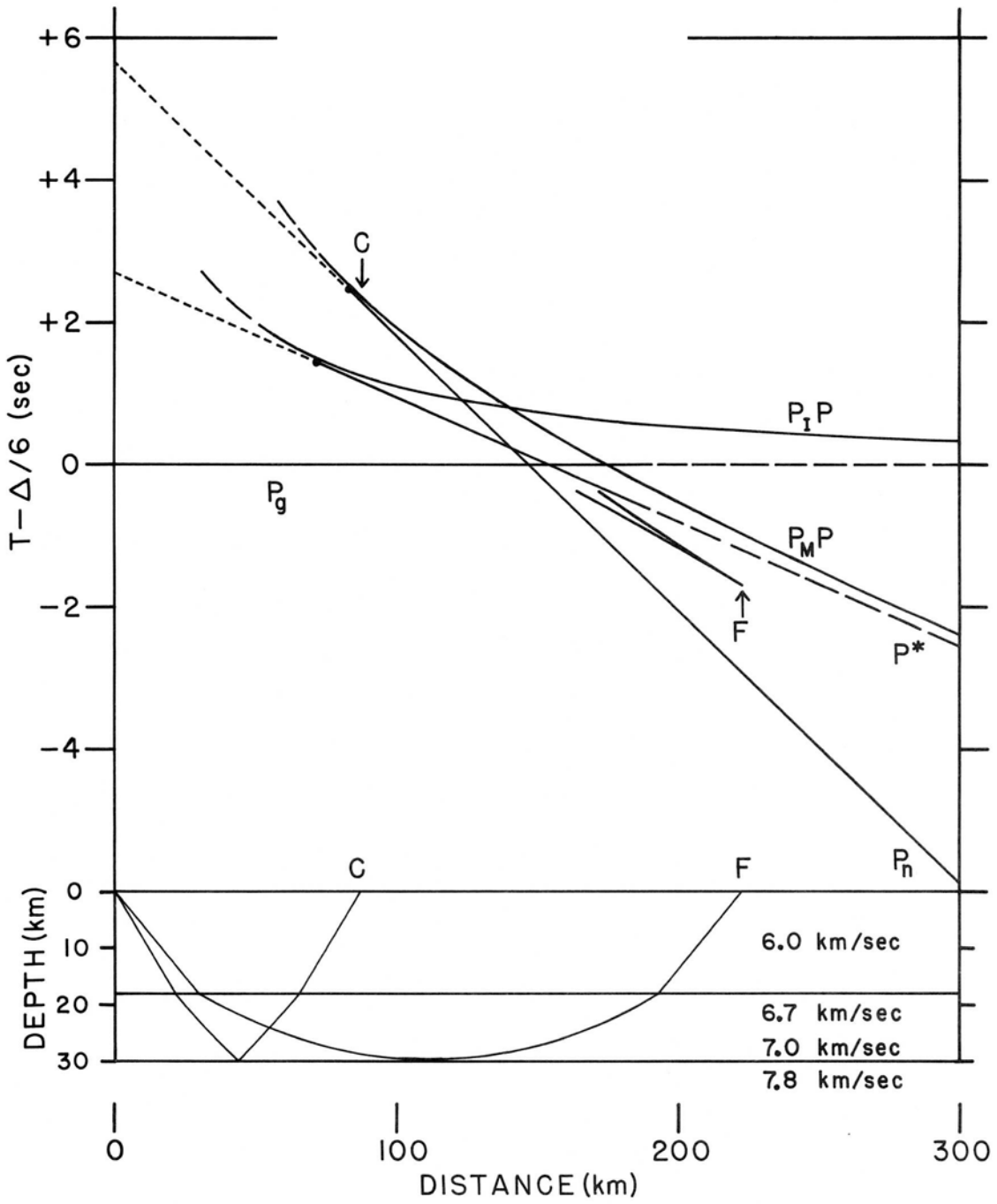

Figure 5.-- Reduced traveltime diagram and critical ray paths for a two-layer crustal model. In the upper part of the diagram, traveltime curves are drawn for the principal reflected and refracted waves through the structure: $V_1 = 6.0$ km/sec, $0 \leq z < 18$ km; $V_2 = 6.7$ km/sec, $18 \leq z < 30$ km; $V_3 = 8.0$ km/sec, $z \geq 30$ km. P_g is the direct wave through the upper layer, and P* and P_n are waves refracted along the tops of the intermediate layer and the mantle, respectively. $P_I P$ is the reflection from the top of the intermediate layer, and $P_M P$ that from the top of the mantle. An increase in the velocity from 6.7 km/sec at the top of the second layer to 7.0 km/sec at its bottom, as suggested in the lower part of the diagram, changes the traveltime curve considerably. $P_M P$ arrives earlier but does not continue beyond F, at which point it has a ray in common with a wave refracted through the second layer. P* probably still exists for short period waves.

P_IP is tangent to the P* line where both have the critically-reflected ray in common; and at great distances P_IP is asymptotic to P_g. P_MP is tangent to the P_n line where both have in common the ray which was critically reflected from the mantle; and at great distances P_MP is asymptotic to P*.

If velocity increases with depth in a layer the foregoing relationships are altered somewhat, as was shown by A. Mohorovicic (1910) many years ago. To illustrate this point, assume that the velocity in the intermediate layer increases linearly from 6.7 km/sec at its top to 7.0 km/sec at its bottom. Then, as is suggested in the sketch below the traveltime diagram (Fig. 5), there is one ray which grazes the bottom of the intermediate layer and returns to the surface at F. This arrival is common to both the wave refracted through the intermediate layer and the one reflected from the top of the mantle (P_MP). Both of these waves, according to ray theory, are terminated at F. Ray theory cannot predict changes in the behavior of waves such as P* and P_n which are critically refracted along layer boundaries, however.

Several changes in the traveltime curves would result from this change in structure. P_n would arrive slightly earlier, and the position of the ray critically reflected from the mantle would be changed slightly. Most important, the wave reflected from the mantle would be terminated at a distance of about 220 km and a wave refracted through the intermediate layer would arrive along a curve joining F (at the point of the hanging cusp on the traveltime diagram) and the point at which P_IP is tangent to P*.

P* would probably still exist, at least in the limit for high-frequency waves. Because P* for this structure never is a first arrival and because its amplitude (by analogy with P_n) is probably small, it might not be easily identifiable on the seismogram.

Seismic profiles: traveltimes and amplitudes of observed waves and structure of the crust. The primary data on waves observed along the five profiles treated herein are summarized graphically in the traveltime plots (Figs. 6-10) and in the amplitude plots (Figs. 11-15). Points representing arrival times of a wave at the seismometers on a spread nearest and farthest from the shotpoint are connected by a short line, the slope of which indicates the apparent velocity of the wave across the spread.

Initial effort was concentrated on first arrivals, and traveltime lines for P_g and P_n were drawn. Then later arrivals, which include the largest waves on the seismogram, were considered. In correlating a phase from one spread to the next, its apparent velocity and amplitude as well as its traveltime were taken into account.

Amplitudes of all phases timed on the seismogram were determined as described earlier. All measured amplitudes were scaled to those expected from a 2000 lb. shot on the assumption that amplitude is proportional to the charge size. For a selected set of waves on each profile, log amplitude was plotted vs distance (Figs. 11-15). These amplitude graphs should be considered in assessing the reliability of secondary phases which have been identified on the traveltime plots.

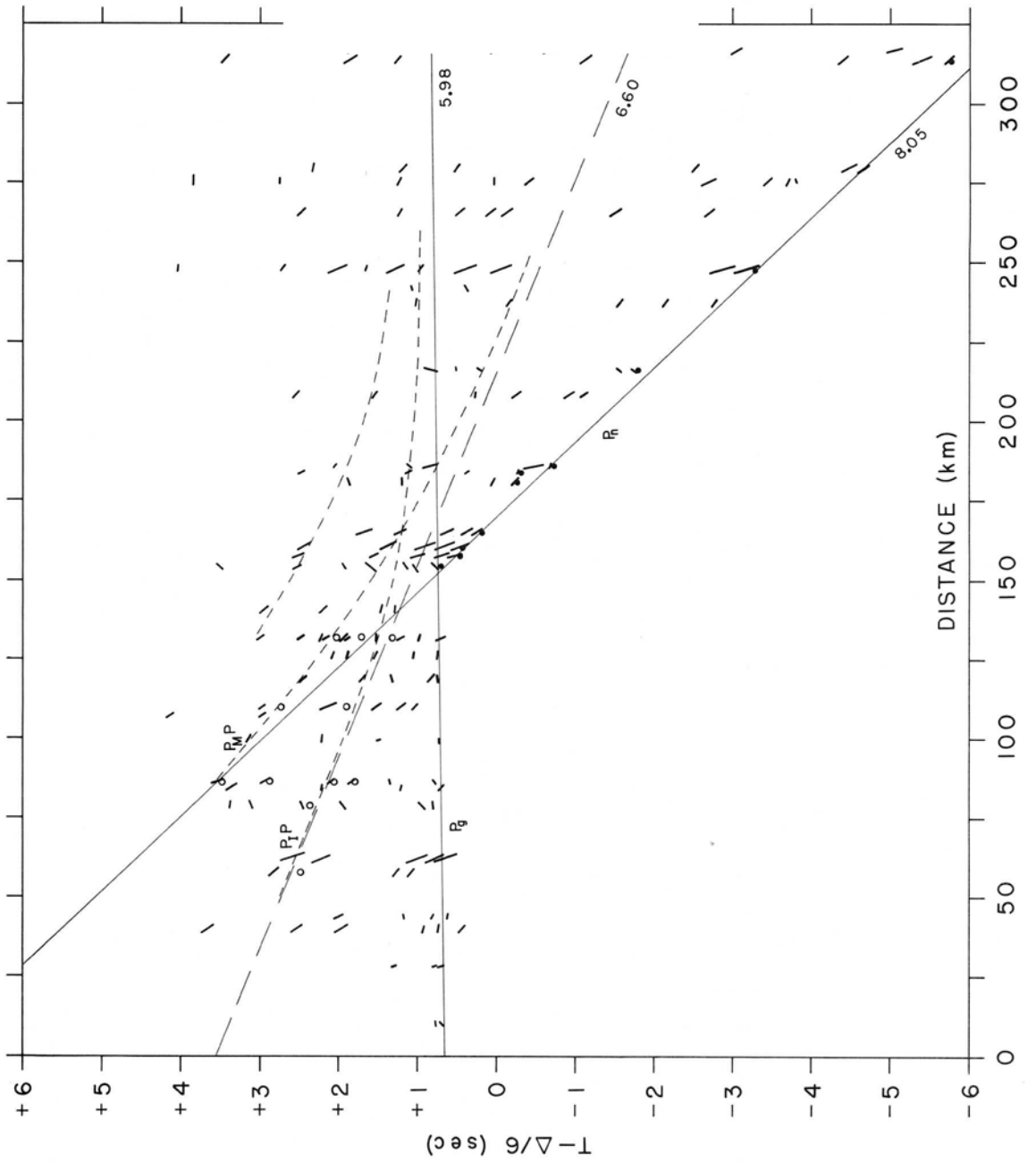

Figure 6.-- Reduced traveltime graph: Eureka to Fallon. Traveltimes of a phase to the nearest and farthest receiver on a spread are connected by a line, the slope of which indicates the apparent velocity of the phase across the spread. P_n arrivals corrected for elevation of the receiver are plotted as solid circles. $P_I P$ and $P_M P$ arrivals corrected for excess delay in near-surface materials are plotted as open circles. The velocity, in km/sec, indicated by a traveltime line is given at its right-hand end. The same conventions are used on Figures 7-10.

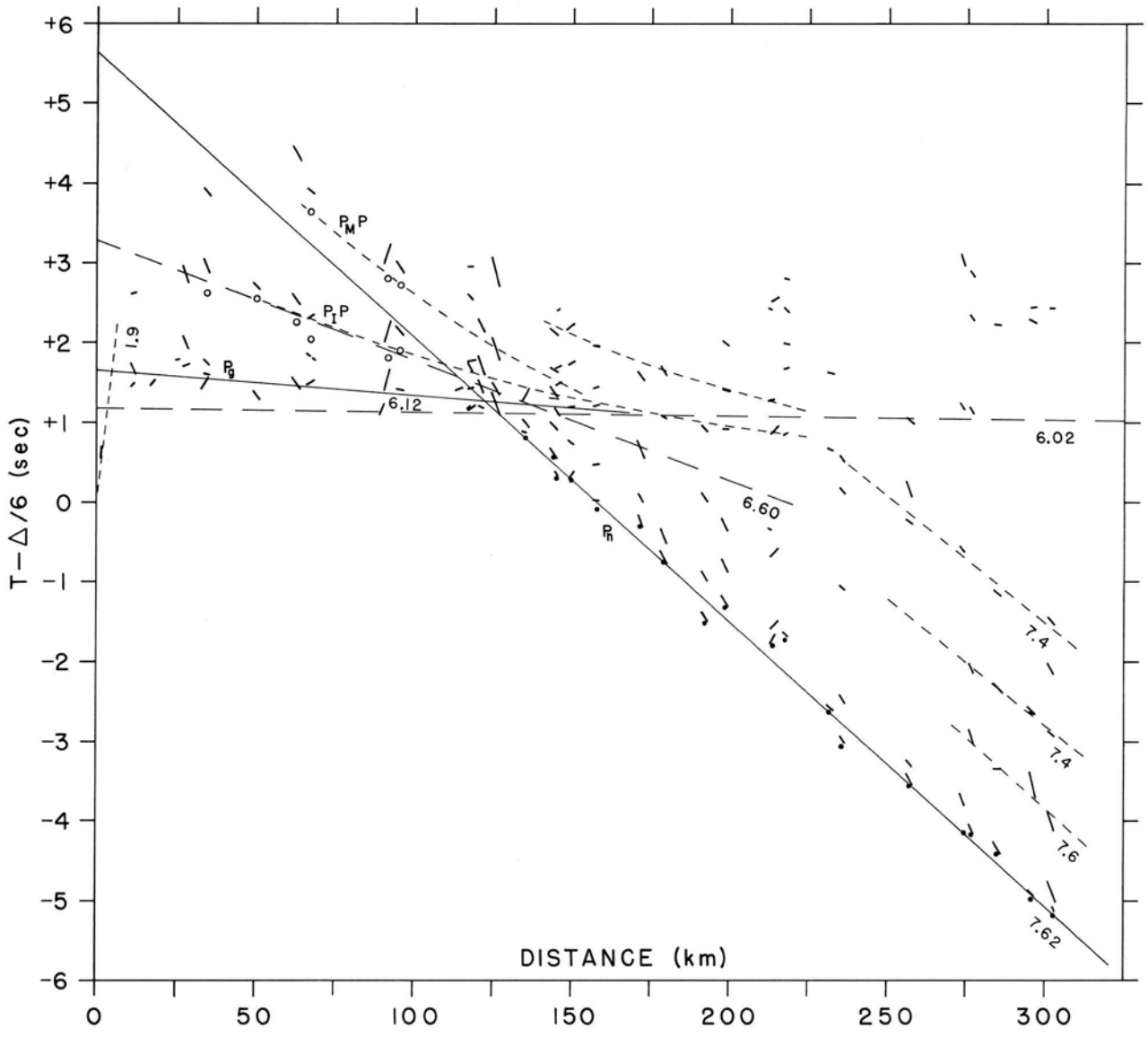

Figure 7.-- Reduced traveltime graph: Fallon to Eureka.

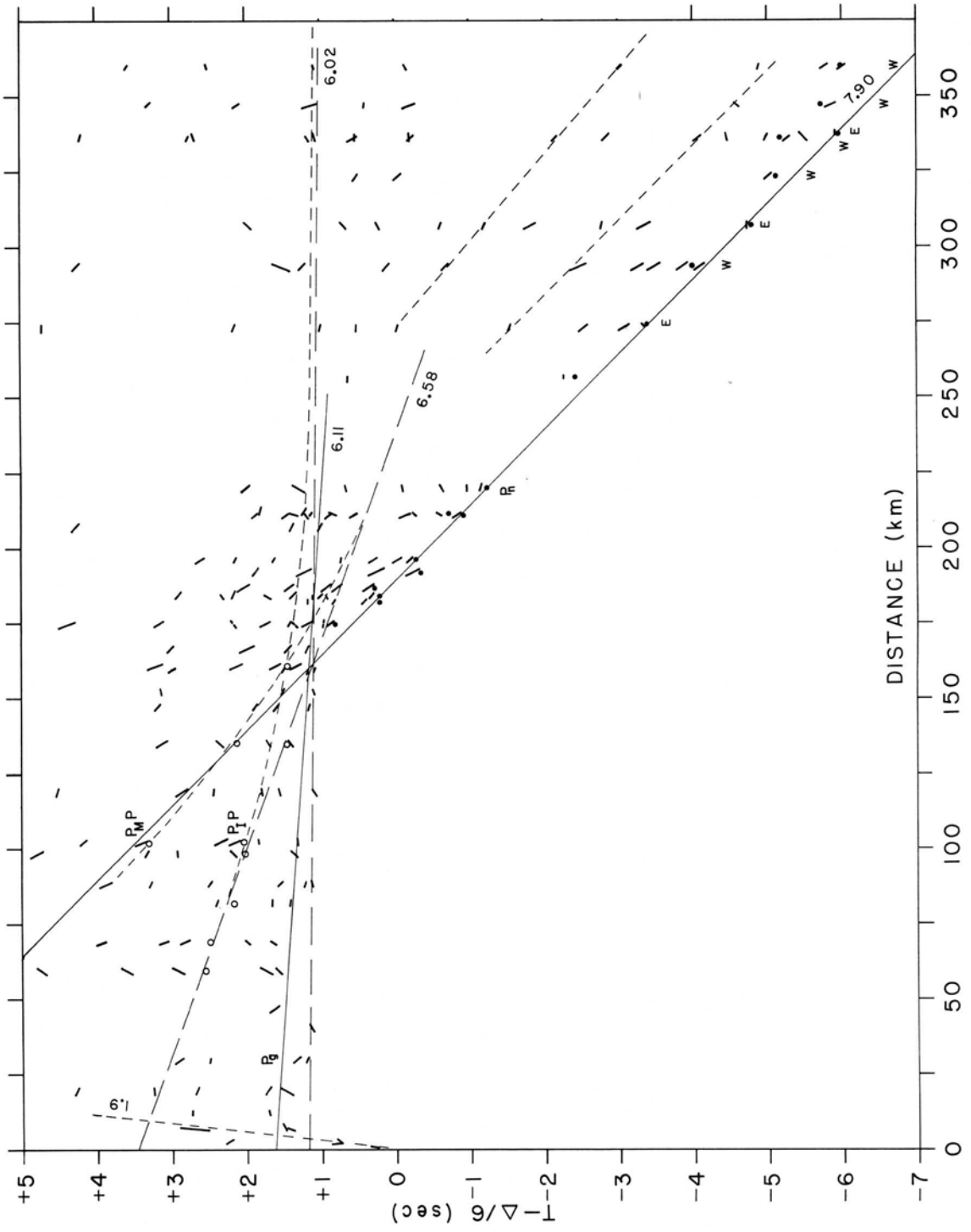

Figure 8.-- Reduced traveltime graph: Fallon to Owens Valley. Beyond 250 km, spreads marked E were recorded along the east flank of the Sierra and those marked W, along the west flank.

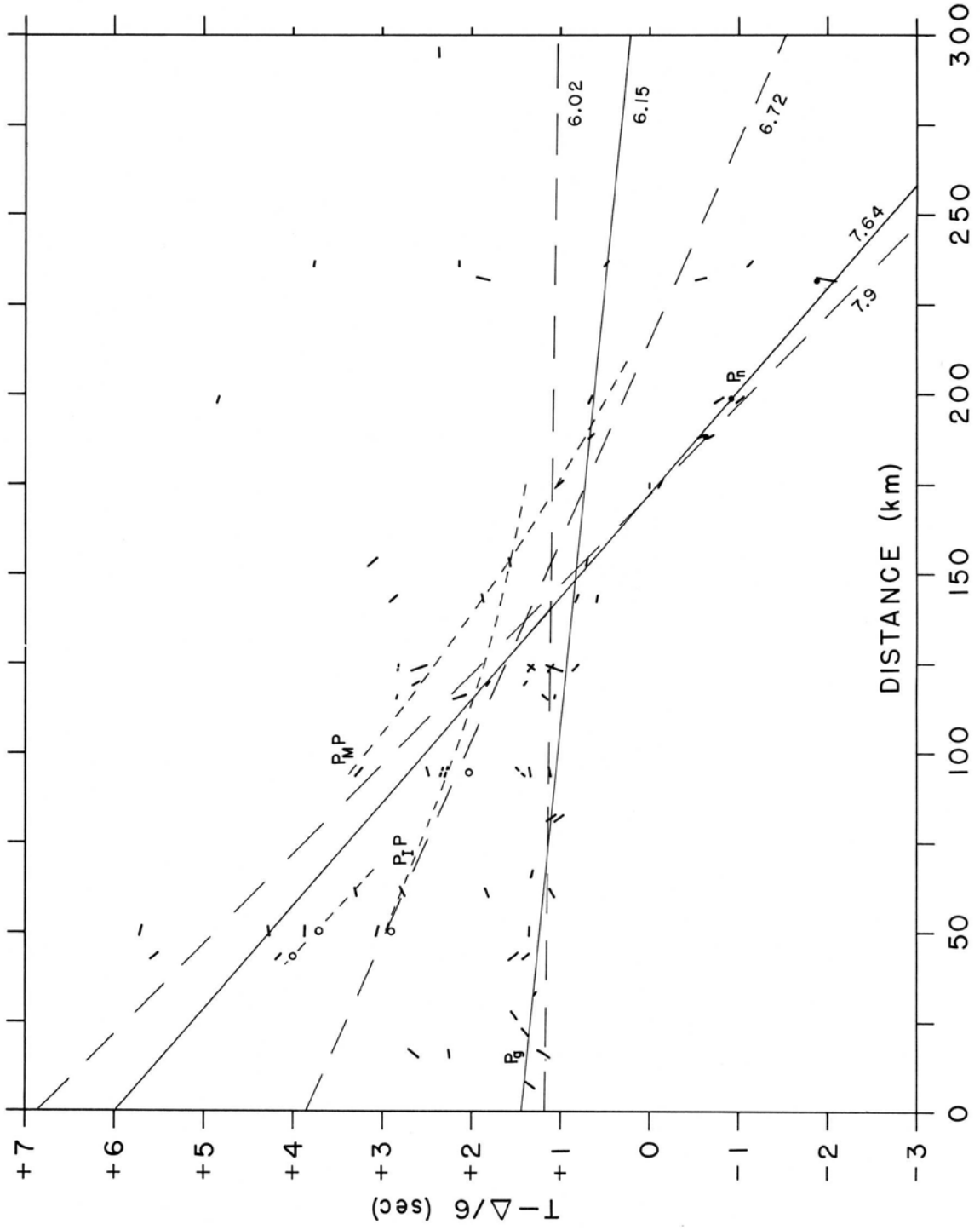

Figure 9.-- Reduced traveltime graph: Fallon to San Francisco.

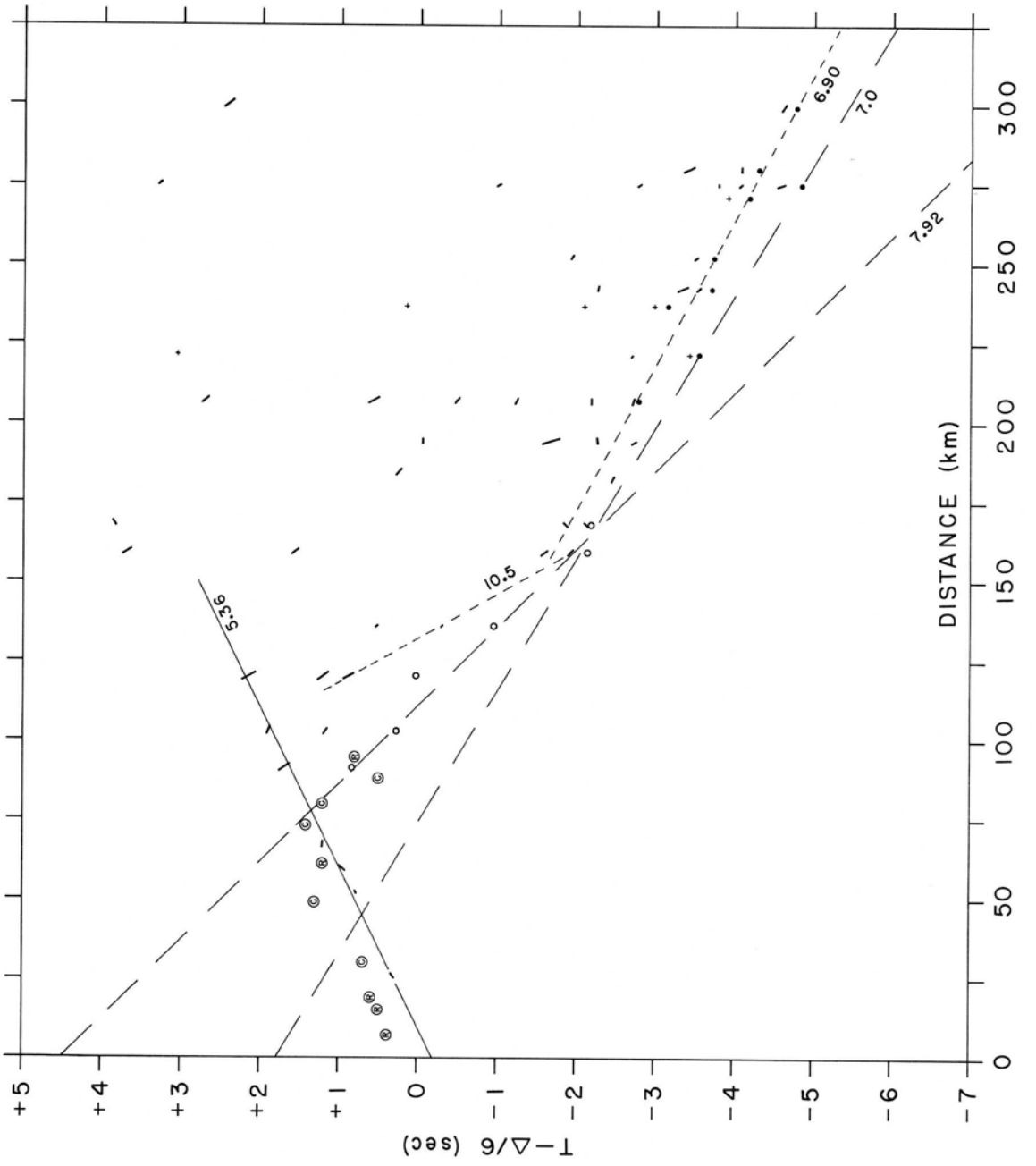

Figure 10.-- Reduced traveltime graph: San Francisco to Fallon. P_n arrivals corrected for elevation of the receiver are plotted as solid circles; when corrected for abnormal delay in sediments of the Great Valley, P_n arrivals are plotted as open circles. R represents a first arrival from the Richmond Quarry blasts; C, from the Port Chicago explosion. A "+" represents an arrival at a spread on which only one seismometer gave a useable record.

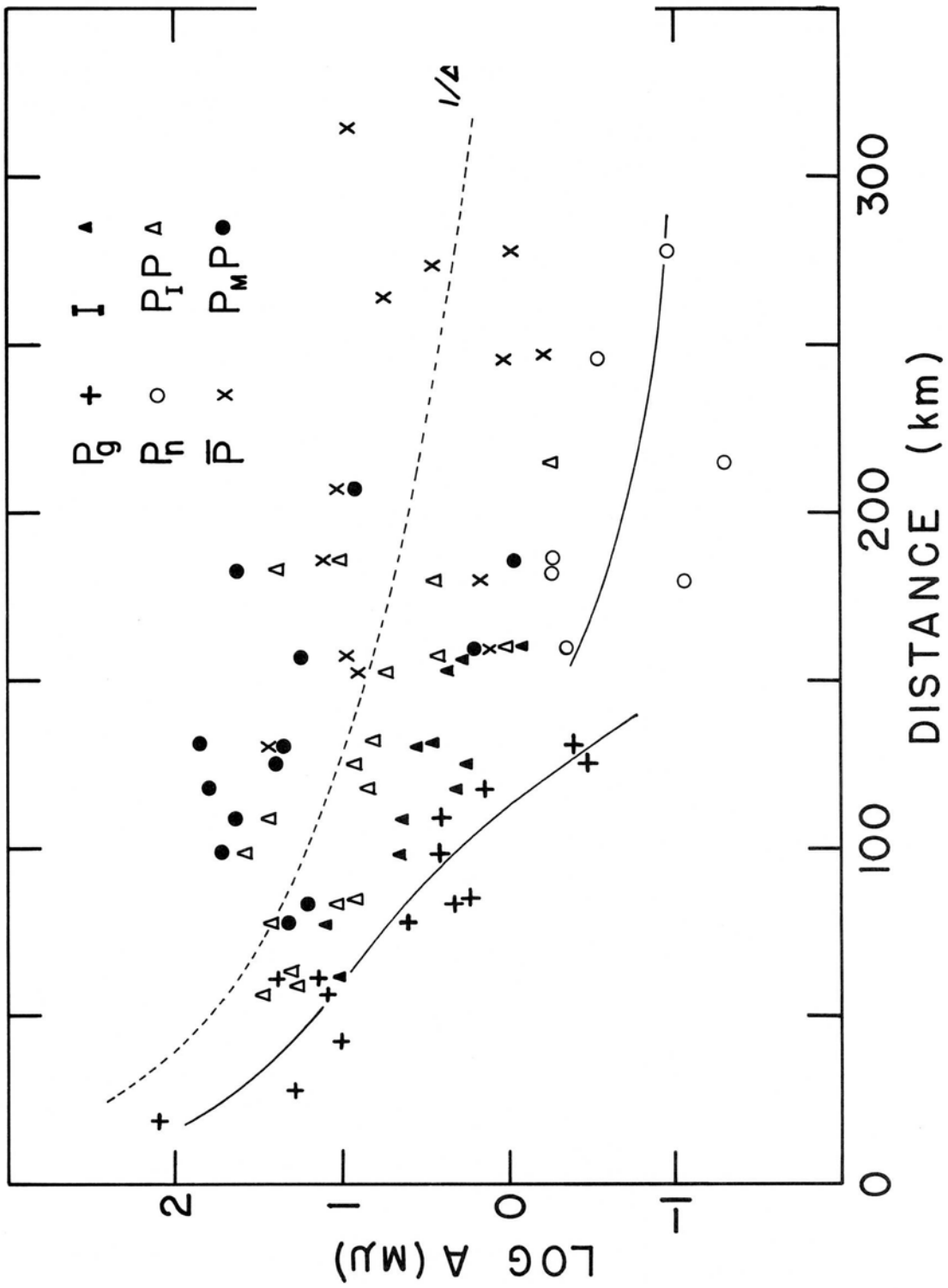

Figure 11.-- Amplitude vs distance: Eureka to Fallon. Log A is plotted vs distance (km), where A is the ground displacement (1/2 peak to trough) expressed in millimicrons. The solid curves were drawn by inspection through P_g and P_n. The dashed line is a reference line showing the law $A \propto \frac{1}{\Delta^2}$, where Δ is distance: it is the same on Figures 11-15.

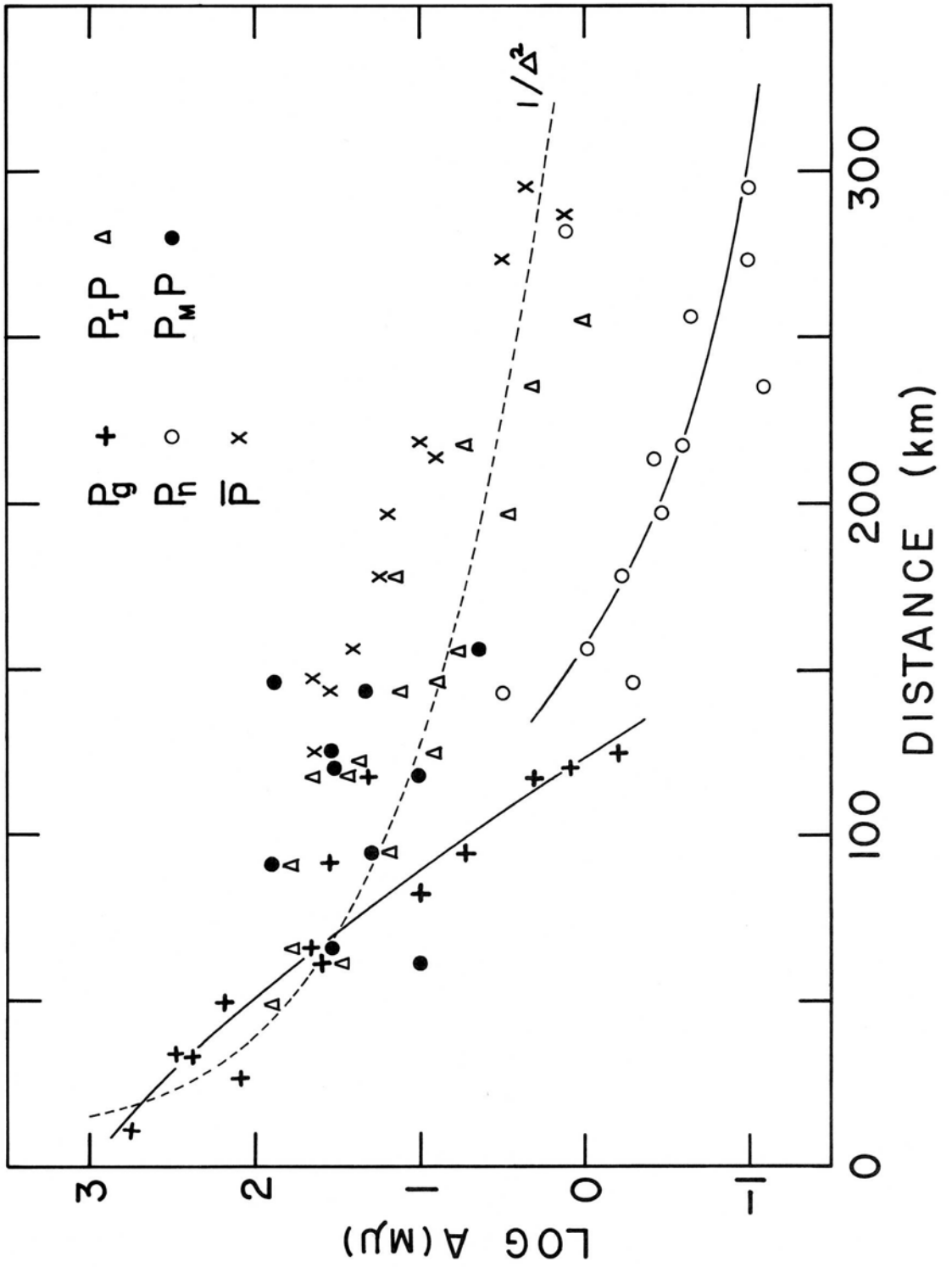

Figure 12.-- Amplitude (1/2 peak to trough) vs distance: Fallon to Eureka.

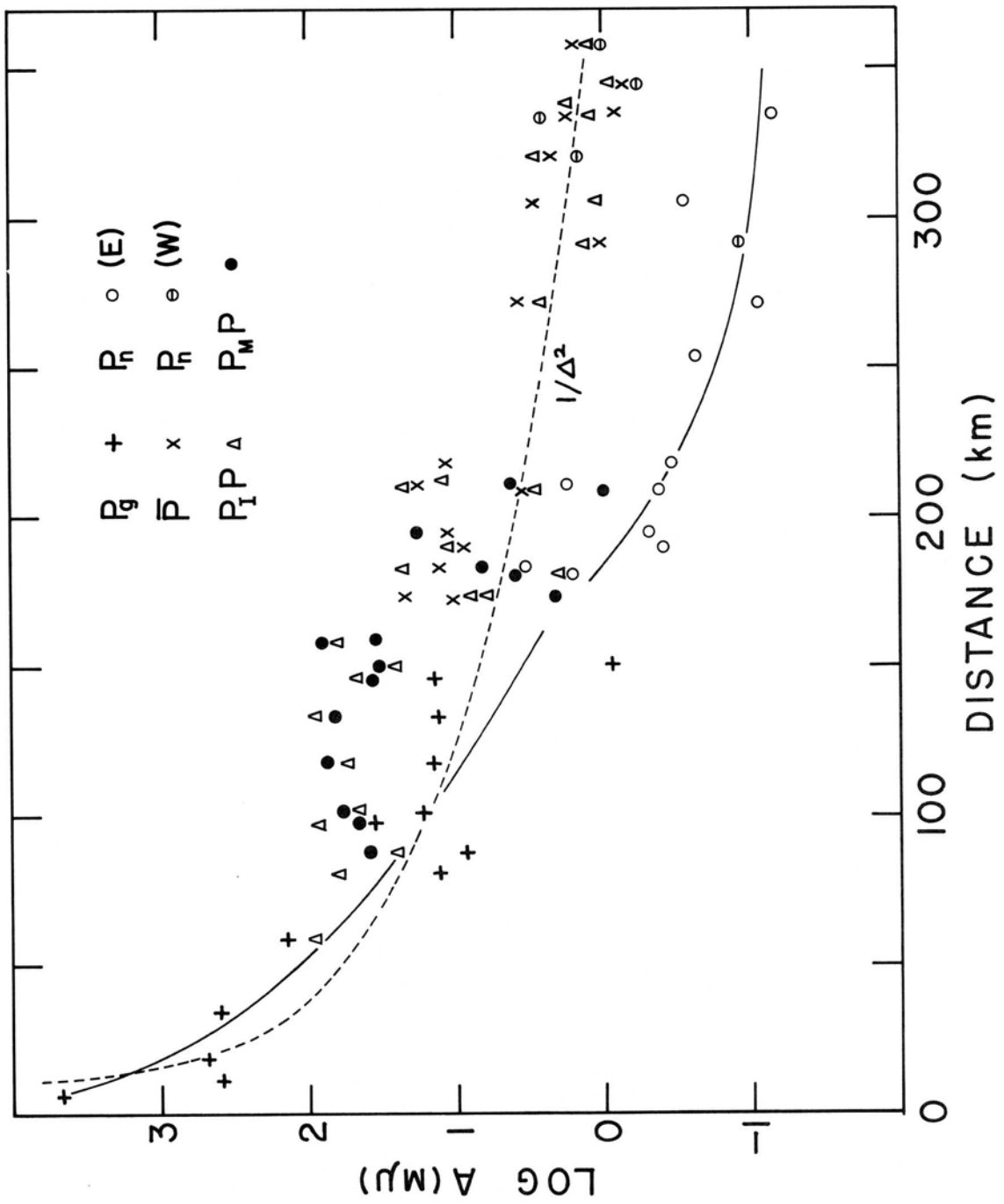

Figure 13.-- Amplitude (1/2 peak to trough) vs distance: Fallon to Owens Valley.

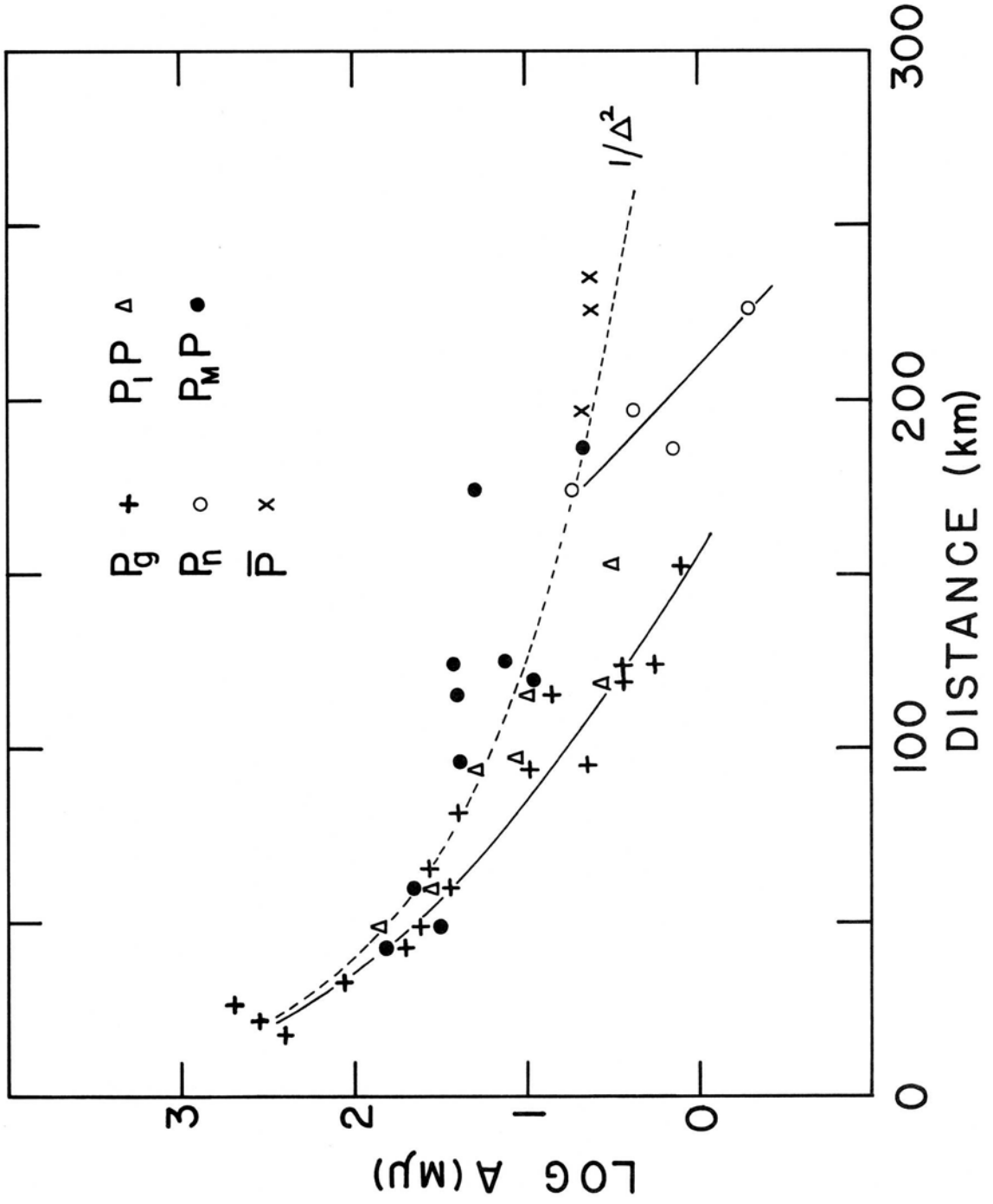

Figure 14.-- Amplitude (1/2 peak to trough) vs distance: Fallon to San Francisco.

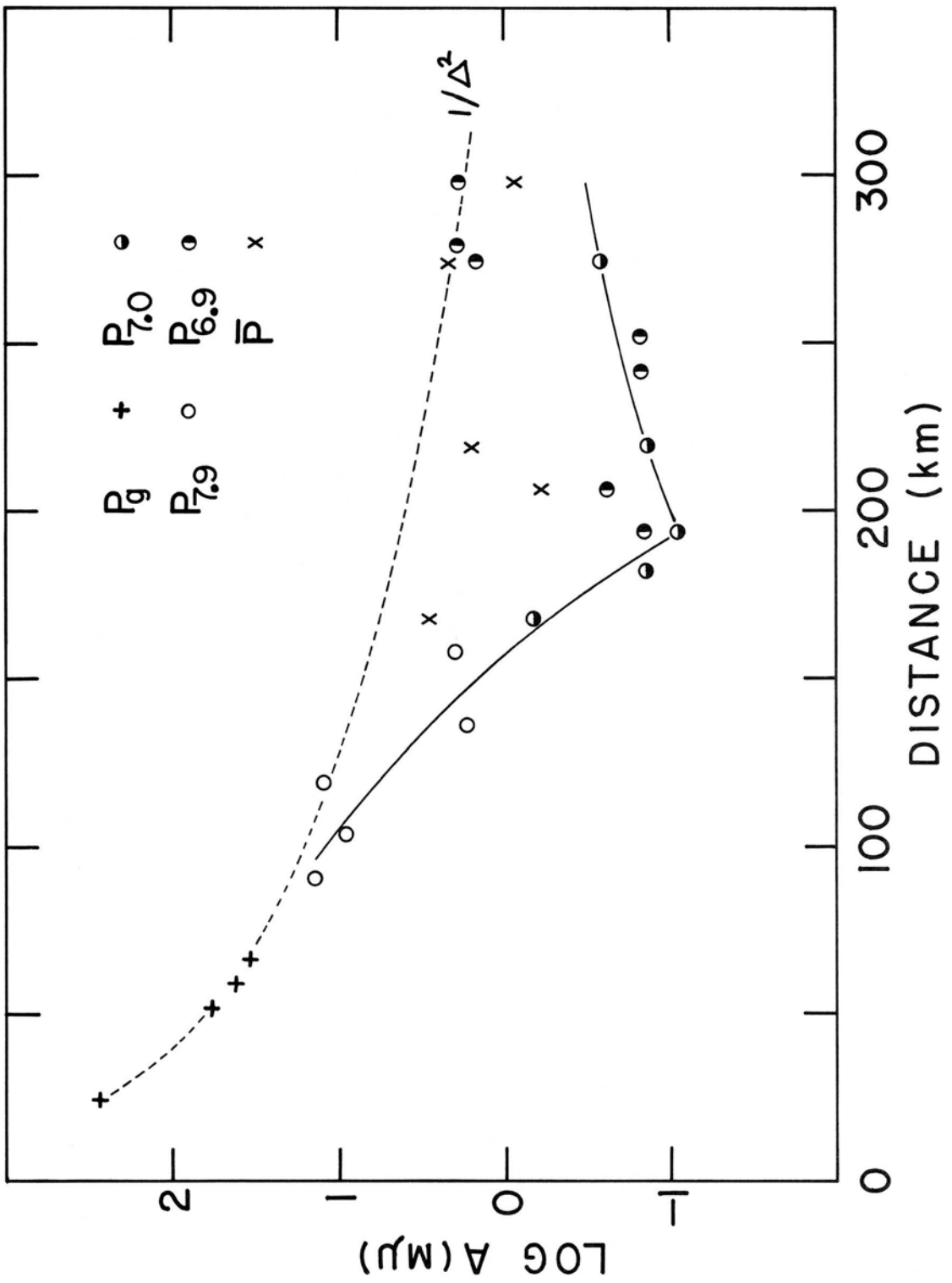

Figure 15.-- Amplitude (1/2 peak to trough) vs distance: San Francisco to Fallon.

Basin and Range. The principal waves recorded on profiles in the Basin and Range province from shotpoints at Fallon and Eureka are sufficiently similar that a single description will cover all profiles. The San Francisco to Fallon profile presents several unique problems which will be dealt with separately.

P_g recorded along profiles from Fallon and Eureka has a velocity near 6.0 km/sec and is the first arrival from a distance of less than 10 km to that at which P_n emerges ahead of it between 130 and 170 km. Its amplitude falls off rapidly with distance (though rather erratically along sections of some profiles (Fig. 13)). If the P_g amplitude-distance curve is projected to distances where P_n is the first arrival, it appears that P_g is smaller than P_n and that it would not be observed as a later arrival. Similar results are reported by Healy (1963) for profiles between San Francisco and Santa Monica, California, and by Ryall and Stuart (1963) for the profile from the Nevada Test Site to Ordway, Colorado. Beyond the P_g-P_n crossover, the largest waves on the seismogram generally appear within one or two seconds after the projected P_g travel-time line (Fig. 2). Apparent velocities of these large waves tend to be greater than that of P_g. Such velocities, coupled with later arrivals, suggest that these are not simple, direct waves. It appears that several different "paths" contribute to these arrivals, which were grouped under the term $\overline{P}$. (Healy, 1963; Ryall and Stuart, 1963).

The wave refracted along the top of the mantle, P_n, is the first arrival from the P_g-P_n crossover between 130 and 170 km to the end of the profiles at about 300 km. Its intercept and apparent velocity vary considerably from profile to profile. Such variations can be explained by changes in crustal structure and by a slight decrease in the velocity at the top of the mantle from the western margin of the Basin and Range province toward its center. Amplitudes of P_n recorded in the Basin and Range province are uniformly small and appear to diminish with distance as about $1/\Delta^2$. Scatter in P_n amplitudes was too severe and the distance over which this phase was recorded too small to justify a more rigorous analysis of the P_n amplitude-distance relationship.

No wave refracted from the top of an intermediate layer produced first arrivals on the Basin and Range profiles discussed here.

From about 60 km to the P_g-P_n crossover, the largest arrivals on the seismogram followed P_g by a fraction to about 3 seconds. On the traveltime plots (Figs. 6-9) these arrivals fall into two groups: one appears to represent a wave reflected from the top of an intermediate layer (P_IP, Fig. 2) and the other, from the top of the mantle (P_MP, Fig. 2). If this interpretation is correct, we should be able to estimate the position of the traveltime line of the "masked" refraction from the intermediate layer. Referring to Figure 5, for a two-layer crust with constant velocities throughout each layer the traveltime line for the intermediate layer refraction (P*) is tangent to P_IP at the critical point and is the asymptote approached by P_MP at large distances.

As actually observed, P_IP appears to approach the P_g line asymptotically and to retain large amplitudes to great distances (Figs. 6, 7, 8, 11, 12, 13). The P_MP curve has its beginning near the P_n line extended toward the shotpoint, and the amplitude of this phase is extremely large on most profiles from 60 or 80 km to the P_n-P_g crossover. Although the trend of the P_MP line suggests this phase should be recorded between P_n and $\overline{P}$ beyond the crossover, it is generally small in this range, and it cannot be identified with confidence beyond about 200 km. The rapid disappearance of P_MP with increasing distance leaves it somewhat in doubt that this phase actually "crosses" P_IP and P_g. A slight increase in velocity with depth within the intermediate layer should cause P_MP to disappear beyond a limiting distance.

On the traveltime plots, corrections for near-surface delays and for variation in receiver elevation were carried out only for arrivals of keen interest such as P_n, P_g, P_IP, and P_MP. A solid circle beside an arrival (P_n only) on the traveltime plots indicates the correction for receiver elevation. Open circles near arrivals on P_MP or P_IP indicate corrections for near-surface delays in excess of that for an average receiver. These corrections are based on P_g delays at the spreads in question and were obtained from Figure 4. At distances beyond 100 km P_g tends to be very weak. If P_g is picked late, the corresponding corrections for P_IP and P_MP will be excessive.

Equations for traveltime curves of P_g, P_n, and P*(?), the latter curve drawn to satisfy the appropriate relationships with P_IP and P_MP, were determined from the traveltime graphs (Figs. 6-9). The observed curves were then corrected for near-surface delays beneath the shotpoint, δT_s, and beneath the average (range) receiver, $\overline{\delta T_R}$. The thicknesses of low-velocity materials beneath the shotpoint, h_s, and beneath the average (range) receiver, $\bar{h}_R$, as well as the corresponding delays for P_n and P*(?) were obtained from Figure 4 on the basis of the P_g delays already deduced for those locations.

At the Eureka shotpoint the P_g delay was 0.33 second; and the P_g delay beneath the average range receiver west of Eureka was 0.33 second. Although the P_n observations from Eureka were made beyond the region where the foregoing receiver delay was determined, they were obtained primarily on ranges in a region of similar geology. An average receiver P_g delay of 0.33 second was assumed for the spreads that recorded P_n from shots at Eureka. From the P_g delays adopted for the Eureka to Fallon profile, $h_s = \bar{h}_R = 0.72$ km.

At the Fallon shotpoint the P_g delay was 0.88 second; and the P_g delay beneath the average range receiver on profiles from Fallon was 0.30 second. The same average P_g delay, 0.30 second, was assumed for spreads recording P_n from shots at Fallon. From the P_g delays adopted for profiles from Fallon, $h_s = 2.41$ km and $\bar{h}_R = 0.65$ km.

Traveltime data from profiles in the Basin and Range province are summarized in Table I.

Table I--Traveltime data from Basin and Range Profiles.

		Observed TT curves	δ_{T_s}	$\overline{\delta T}_R$	Corrected TT curves
Eureka	P_g	0.66 +Δ/5.98	0.33	0.33	Δ/5.98
to	P*(?)	3.58 +Δ/6.60	0.25	0.25	3.08 +Δ/6.60
Fallon	P_n	7.23 +Δ/8.05	0.25	0.25	6.73 +Δ/8.05
Fallon	P_g(av)	1.65 +Δ/6.12			
to	P_g(range)	1.18 +Δ/6.02	0.88	0.30	Δ/6.02
	P*(?)	3.28 +Δ/6.60	0.68	0.23	2.37 +Δ/6.60
Eureka	P_n	5.62 +Δ/7.62	0.65	0.23	4.74 +Δ/7.62
Fallon	P_g(av)	1.63 +Δ/6.11			
to	P_g(range)	1.18 +Δ/6.02	0.88	0.30	Δ/6.02
Owens	P*(?)	3.45 +Δ/6.58	0.68	0.23	2.55 +Δ/6.58
Valley	P_n(E)	7.58 +Δ/7.90	0.65	0.23	6.70 +Δ/7.90
Fallon	P_g(av)	1.44 +Δ/6.15			
to	P_g(range)	1.18 +Δ/6.02	0.88	0.30	Δ/6.02
San	P*(?)	3.85 +Δ/6.72	0.68	0.23	2.94 +Δ/6.72
Francisco	P_n (velocity assumed)	6.87 +Δ/7.90	0.65	0.23	5.99 +Δ/7.90

An additional arrival on the Eureka to Fallon profile (Fig. 6) is a small but distinct phase that precedes $P_I P$ by about 0.4 second from 60 km to the P_g-P_n crossover. The amplitude of this phase (designated by I) is plotted vs distance in Figure 11. It might represent a wave reflected from a horizon in the crust above that responsible for $P_I P$.

Several features of the Fallon to Eureka traveltime graph (Fig. 7) beside those summarized in Table I deserve mention. Between 250 and 300 km three sets of arrivals with velocities near that of P_n follow P_n after intervals of 1.2, 2.3, and 3.5 seconds. Clusters of abnormally prominent arrivals in the $\overline{P}$ region of the traveltime graph at distances of approximately 145 km, 215 km, and 280 km suggest repeated reflections of energy near the critical angle from the top of the intermediate layer. The half-second lag of (corrected) $P_M P$ arrivals with respect to the extension of the P_n line suggests a change in the inclination of the top of the mantle east of Fallon: i.e., it seems that the eastward dip of the mantle begins (or increases) about 50 km east of the shotpoint.

Fallon to Eureka. Crustal structure between Fallon and Eureka was computed by the standard "dipping bed" refraction equations (Mota, 1954) from the corrected traveltime curves for these two profiles. These equations assume plane, continuous boundaries from shotpoint to shotpoint along the profile.

For the velocity of P in the principal crustal layer, the mean of the Eureka and Fallon P_g velocities, 6.00 km/sec, was adopted. Neglecting the possible intermediate layer, the mantle dips from Fallon

toward Eureka at an angle of 1.7° and has a P velocity of 7.82 km/sec. The depth to the mantle beneath Fallon is 22.2 km and beneath Eureka, 31.5 km.

If the intermediate layer is present, it has a velocity of 6.6 km/sec and dips from Fallon toward Eureka at an angle of 1°. Beneath Fallon it lies at a depth of 17.2 km and beneath Eureka, at 22.3 km. The top of the mantle has a velocity of 7.82 km/sec and dips from Fallon toward Eureka at an angle of 2°. It lies 24.1 km beneath Fallon and 33.9 km beneath Eureka. Both interpretations result in a surprisingly thin crust beneath the Fallon shotpoint. Soda Lake, in which the shots were detonated, may be underlain by intrusive rocks of abnormally high velocity. The thin crust here ascribed to the Fallon shotpoint may be of limited horizontal extent.

Fallon to Owens Valley. The reflected phases P_IP and P_MP, were especially prominent on the profile from Fallon to Owens Valley (Figs. 8 and 13). P_n arrivals beyond 250 km on this profile were recorded both along the east side of the Sierra north of Owens Valley and on the west flank of the Sierra north of Portersville. Only arrivals east of the Sierra were considered in drawing the P_n traveltime line. Arrivals on the west flank of the Sierra, though large in amplitude (Fig. 13), are delayed between 0.2 and 0.9 second with respect to this line.

Because this profile was not reversed and because observed wave velocities were not extreme, an average crustal structure along it was calculated on the usual assumptions of constant layer velocities and flat-lying boundaries between layers.

Disregarding the possible intermediate layer, the average thickness of the crust (velocity 6.02 km/sec) along the profile is 31.1 km. If the single-layer Fallon crust obtained from the Eureka-Fallon profile is adopted for the shotpoint, then the crust must be thickened to 40.0 km beneath the profile north of Owens Valley.

If the intermediate layer is accepted as real the average thickness of the first layer (velocity 6.02 km/sec) is 19.0 km, and that of the second layer (velocity 6.58 km/sec) is 15.5 km, for a crustal thickness of 34.5 km. On the assumption that the 2-layer Fallon crust obtained from the Eureka-Fallon profile is the actual structure at the shotpoint, the depth to the intermediate layer is 20.8 km and that to the Moho is 44.9 km north of Owens Valley. Because P_MP is observed within 100 km of Fallon and because it lies along the P_n line determined by arrivals along the south half of the profile, the principal thickening of the crust along this profile must occur less than 50 km south of Fallon.

The average delay of P_n at the four most distant trans-Sierra receivers is 0.6 second. If this delay is caused by a simple thickening of the "granitic" crust at the expense of the mantle, the crust beneath the high central part of the Sierra is about 7 km thicker than it is north of Owens Valley, or about 50 km thick.

Fallon to San Francisco. On the profile from Fallon to San Francisco, three arrivals between 40 and 65 km might be due to P_MP from the shallow mantle beneath Carson Sink. A series of good arrivals falling above the extension of the P_n line appears to represent P_MP from 90 to 200 km. Other interpretations are possible for some of the arrivals on this curve.

Observed P_n arrivals over a range of 60 km just west of the Sierra crest determine a velocity of only 7.64 km/sec. Because this profile was not adequately reversed, the dip of the Moho and the upper mantle velocity along it cannot be calculated. To obtain an estimate of the average crustal structure west of Fallon, a line was drawn through the P_n arrivals near the P_g-P_n crossover with a slope corresponding to the P_n velocity observed on the Fallon to Owens Valley profile, 7.90 km/sec.

Neglecting the possible intermediate layer, the average thickness of the crust along this profile is 31.1 km. If the structure at Fallon determined from the Eureka-Fallon profile (1-layer crust) is accepted for the shotpoint, the thickness of the crust beneath the Sierra west of Fallon is 40.0 km.

If the intermediate layer is not neglected, the average depth to its upper surface is 19.9 km and the depth to the mantle is 33.7 km. For the two-layer crust beneath the shotpoint obtained from the Eureka-Fallon profile, the depths to the intermediate layer and to the mantle beneath the Sierra west of Fallon must be 22.1 km and 42.8 km, respectively.

On the evidence of the interruption of P_MP between 65 and 90 km, it appears that the crust thickens abruptly about 40 km west of Fallon.

San Francisco to Fallon. The profile from San Francisco to Fallon presents several unusual difficulties. The shotpoint in the Pacific Ocean 25 km southwest of Golden Gate is about 20 km west of the San Andreas fault, along which large strike slip has occurred in Cenozoic time. Along the San Andreas in central California, a terrain with granitic basement rocks on the west has been brought into contact with one with a Franciscan basement on the east (King, 1959). It appears that the fault is a profound feature along which the entire sialic crust on one side of the fault has been displaced a large distance with respect to that on the other side.

The receiver nearest the shotpoint was in Golden Gate Park, east of the San Andreas, above a Franciscan basement. The next three receivers were in the Berkeley Hills east of San Francisco Bay, still above a Franciscan basement but resting on folded rocks of younger age. The profile then extends onto the deep sediments of the Great Valley in the low-lying "Islands" region of the confluence of the Sacramento and San Joaquin rivers.

Depth to basement in this region might exceed 30,000 feet (Bowen, 1963). High noise levels from agricultural activities, moreover, made recording very difficult. Eastward the depth to basement diminishes rapidly, until it outcrops in the western foothills of the Sierra Nevada. Farther east, the ground surface rises to great heights: a critical low-noise recording was obtained at 7,300 feet near Lake Tahoe.

If corrections are applied only for ground-surface elevation, the first arrivals determine the following traveltime lines: 25 to 90 km, $T = -0.20 + \Delta/5.36$ sec; 120 to 160 km, apparent velocity 10.5 km/sec; and 160 to 275 km, $T = 1.96 + \Delta/7.04$ sec.

Generally low crustal P velocities in central California have been recognized by Byerly (1939) for many years. First arrivals from quarry blasts at Richmond recorded east of the San Andreas fault and as far south as Mt. Hamilton are plotted on the traveltime curve (Fig. 10) as R (Byerly and Wilson, 1934; Tocher, 1956). The Port Chicago Explosion first arrivals are plotted as C (Byerly, 1946). As the Port Chicago Explosion origin time was somewhat in doubt, a time was chosen so that first arrivals at Berkeley, San Francisco, and Palo Alto conformed to the Richmond Quarry blast traveltimes. From these data it seems clear that the velocity of P through the crust east of the San Andreas in this region is low, not greater than 5.6 km/sec. An intercept of about 0.3 seconds for the crustal P wave is indicated by the Richmond Quarry blast data. First arrivals along the present profile lead those from the Richmond Quarry blast by several tenths of a second. Higher crustal velocities west of the San Andreas are needed to explain this discrepancy. If near-surface delays are the same on both sides of the fault, a crustal velocity of about 6.0 km/sec west of the fault is required. Such a velocity is in general agreement with the results reported by Healy (1963) for the profiles between San Francisco and Camp Roberts, which lie entirely within the area with granitic basement rocks west of the fault.

From geologic evidence the depth to basement beneath the spreads recorded in the Great Valley can be estimated (Bowen, 1962). For the records obtained at ranges of 91 km, 103 km, 120 km, 136 km, 159 km, and 166 km, the depths are $>$30,000 ft., $>$ 30,000 ft., 20,000 ft., 11,500 ft., 3500 ft., and 1500 ft., respectively. P_n delays for such thicknesses of sediments were obtained from Figure 4. Traveltimes to valley receivers, corrected for the near-surface delays in excess of that corresponding to a P_g intercept of 0.3 sec, are plotted as open circles on the traveltime graph (Fig. 10). A line through these points has the equation $T = 4.50 + \Delta/7.92$ sec, not unreasonable for P_n. The large apparent velocity indicated by the "raw" arrivals between 120 and 160 km is removed. First arrivals from the Richmond Quarry blasts and the Port Chicago Explosion at ranges of 80 to 95 km fall close to this curve and support its small intercept and small P_g-P_n crossover distance. Beyond 160 km, the earliest arrivals fall on the line $T = 1.78 + \Delta/7.01$ sec; and a somewhat stronger arrival about 1/2 second later determines a line with a velocity of 6.90 km/sec. The low velocity of first arrivals along this section of the profile appears to be the result of a rapid eastward thickening of the crust beneath the Sierra Nevada.

Amplitudes of first arrivals beyond 90 km fall off rather steeply to a distance of 190 km. At greater distances they increase somewhat. The break in amplitude does not occur at the same distance as the break in velocity.

Calculations of structure from evidence such as is presented above must be arbitrary. Because the shotpoint was in "granitic" terrain and the P_n data were obtained above a "Sierran" basement, a velocity of 6.0 km/sec was assumed for P_g. The Richmond Quarry blast intercept of 0.3 second was adopted for P_g. For P_n the curve based on the corrected Great Valley traveltimes was accepted. For a P_g intercept of 0.3 second, the total near-surface delay of P_n is about 0.24 second. Traveltime curves, corrected for near-surface delays, for this profile are: P_g, $\Delta/6.0$; P_n, $4.26 + \Delta/7.92$.

The average crustal thickness corresponding to these traveltime curves is 19.6 km. Healy reports a thickness at San Francisco along his coastal profile of 23 km. If this thickness is accepted for the crust at the shotpoint, that beneath the Great Valley would be only about 16 km.

To account for the low speed of P_n(?) beyond 160 km by the thickening of material of velocity 6.0 km/sec over that of velocity 7.92 km/sec, the Moho must dip east along the profile at nearly 11°. From the position of the break in the P_n(?) traveltime curve, the thickening appears to begin beneath the valley just east of the line between Sacramento and Stockton; and the slope extends eastward for a distance of at least 115 km. If it continues to the crest of the Sierra (about 140 km from its beginning on the west) it would carry the Moho to a depth of about 45 km.

H. W. Oliver (written communication) offers strong evidence from measurements of gravity that the crust begins to thicken along the eastern margin of the Great Valley rather than along the line suggested by the break in the P_n(?) traveltime curve. As noted earlier, the break in the P_n(?) amplitude curve occurs about 30 km northeast of the break in the traveltime curve. If the edge of the Sierran root were placed to explain the break in amplitudes, it would lie along the eastern margin of the Great Valley, in agreement with results from gravity. Additional seismic data must be obtained before this problem can be pursued farther profitably.

Summary. In the part of the Basin and Range province traversed by profiles reported in this paper, the velocity of P_g is very near 6.0 km/sec. A decrease from 6.02 km/sec at Fallon to 5.98 km/sec at Eureka is suggested by the data, but this decrease is smaller than the corrections to the raw P_g velocities observed near Fallon which are required by an analysis of near-surface P_g delays. Early P_g arrivals from Fallon at receivers in the eastern Sierra Nevada indicate that the velocity of P_g in that province might be somewhat greater than 6.0 km/sec.

The velocity of P_n between Fallon and Eureka, on the basis of the reversed profile between those shotpoints, is 7.8 km/sec. A slightly higher velocity, 7.9 km/sec, was obtained for P_n along the unreversed profile from Fallon to Owens Valley along the eastern edge of the Sierra Nevada.

Two prominent waves which follow the first arrival closely at distances between 50 and 250 km appear to be reflections from an intermediate layer, P_IP, and from the Moho, P_MP. The velocity of P at the top of the intermediate layer (if such a layer does exist) is about 6.6 km/sec, and it might increase to as much as 7.0 km/sec at the bottom of the layer.

On the profile from San Francisco to Fallon, first arrivals between 24 and 70 km support the low crustal P velocities previously reported by Byerly (1939) and by Tocher (1956) for the central Coast Ranges. First arrivals from the Richmond Quarry blasts recorded between 7 and 70 km along a "line" nearly perpendicular to the San Francisco to Fallon profile fall on a traveltime line with a velocity of 5.6 km/sec and an intercept of +0.3 sec. The present data establish a line with a velocity of 5.4 km/sec and an intercept of -0.2 sec. To account for the negative intercept an appeal must be made to Geology. King (1959) stresses the contrast in basement rocks on opposite sides of the San Andreas Fault in this region: granitic on the west and Franciscan on the east. Source, wave paths, and receivers of the Richmond Quarry blast data reported above lay east of the San Andreas in the region of Franciscan basement rocks. The shotpoint and the first 20 km of the San Francisco to Fallon profile lay west of the San Andreas in the region of granitic basement rocks, while all of the receivers were east of the fault. Thus, it appears that the velocity of P in the crust beneath the area underlain by Franciscan basement is 5.4 to 5.6 km/sec, distinctly lower than the 6.0 km/sec observed in the Basin and Range province.

On the other hand, Healy (1963) reports P_g velocities of 6.0 km/sec or greater along the profile from San Francisco to Santa Monica, the entire profile lying west of the San Andreas Fault above a granitic basement. If the velocity of P in the crust is about 6.0 km/sec from the San Francisco shotpoint to the San Andreas Fault and about 5.4 km/sec beyond the fault, and if the near-surface P_g delays on the two sides of the fault are approximately equal, then the observed traveltime curve is the expected one.

When first arrivals in the Great Valley are corrected for the delays expected from the thick, unconsolidated sediments, they establish a P_n traveltime line with a velocity of about 7.9 km/sec. The low apparent velocity of first arrivals recorded beyond the Great Valley indicate that the Moho dips beneath the Sierra. For a 6.0 km/sec crust above a 7.9 km/sec mantle, the apparent dip of the Moho should be about 11° northeastward along the profile. The position of the break in P_n velocity from 7.9 km/sec to 7.0 km/sec indicates that the crust begins to thicken about 35 kilometers west of the eastern margin of the Great Valley. The P_n amplitude curve suggests, however, that thickening begins beneath the eastern margin of the valley.

West of the San Andreas Fault, the crust, if interpreted as a single layer, is about 20 km thick (possibly a few km thicker) and has a P velocity of about 6.0 km/sec (Fig. 16). East of the San Andreas, beneath the Coast Ranges and the western part of the Great Valley, the crust is

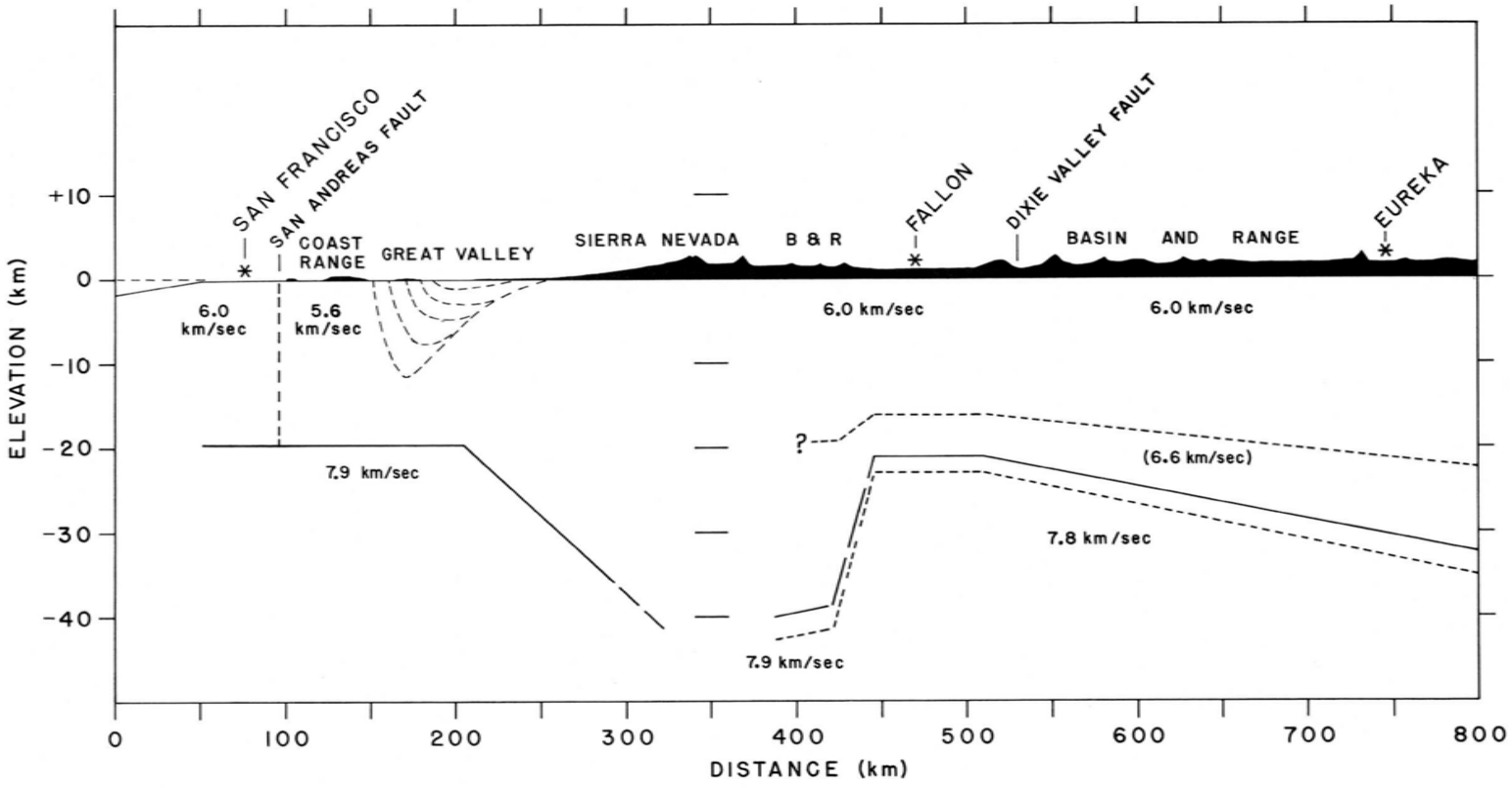

Figure 16.-- Cross section from San Francisco, California, to Eureka, Nevada. The vertical scale is exaggerated 5 times with respect to the horizontal, and the part of the crust above sea level is in black. The heavy solid line depicting the interface between crust and mantle is for the single layer interpretation. East of the Sierra Nevada, the alternate two-layer interpretation is shown by heavy dashed lines. The velocity in parentheses (6.6 km/sec) is that of the possible intermediate layer.

somewhat thinner than 20 km (perhaps as thin as 16 km). The velocity of P in this region of Franciscan basement is low, not greater than 5.6 km/sec. The thick sequence of post-Franciscan sedimentary deposits beneath the Great Valley (Bowen, 1962) displaces approximately half of the crust beneath the western part of the valley. On the east, these deposits are underlain by Sierran basement; on the west, presumably by Franciscan basement. It seems likely that Franciscan rocks of the Coast Ranges compose the entire crust in that region, lying directly on the mantle or on an ancient oceanic crust. Insufficient stewing in the geothermal furnace at great depth, required to raise the metamorphic rank of sediments to that of typical crystalline crust, perhaps explains the low P velocities of these rocks.

East of the middle of the valley the crust begins to thicken rapidly toward the east beneath the Sierra Nevada. At the 11° dip indicated by low P_n velocities recorded up the western slope of the Sierra, the Moho should descend to a depth of 40 to 45 km beneath the high central part of the range. A thicker crust beneath the high Sierra south of this profile is indicated by delays in P_n on the west side of the range from shots at Fallon.

East of the Sierra Nevada, reflected waves indicate that the crust may be composed of two layers; so two interpretations of the traveltime curves are possible. Beneath the Fallon shotpoint in Carson Sink near the western edge of the Basin and Range province, the crust is only 22 km thick according to a single-layer interpretation. It thickens rapidly to about

40 km beneath the Sierra toward the west and beneath the western border of the Basin and Range province adjacent to the Sierra toward the south. From the eastern margin of Carson Sink the crust thickens more gradually toward Eureka, where it attains a thickness of about 32 km.

If we accept the probable intermediate layer indicated by P_IP in the Basin and Range province, total crustal thicknesses are increased by 2 to 5 km.

Acknowledgements. S. W. Stewart performed the original analysis of several of the profiles reported herein. His contributions to the present paper are gratefully acknowledged.

REFERENCES

Bowen, O. E. Jr., editor, Geologic guide to the oil and gas fields of northern California, Bull. 181, California Division of Mines and Geology, 412, p. 1962.

Byerly, Perry, Near earthquakes in central California, Bull. Seism. Soc. Am., 29, 427-462, 1939.

_____, The seismic waves from the Port Chicago explosion, Bull. Seism. Soc. Am., 36, 331-348, 1946.

Byerly, Perry, and James T. Wilson, The Richmond Quarry blast of August 16, 1934, Bull. Seism. Soc. Am., 25, 259-268, 1935.

Hafner, W., The seismic velocity distribution in the Tertiary basins of California, Bull. Seism. Soc. Am., 30, 309-326, 1940.

Healy, J. H., Crustal structure along the coast of California from seismic-refraction measurements, (this symposium), 1963.

Jackson, W. H., S. W. Stewart, and L. C. Pakiser, Crustal structure in eastern Colorado from seismic-refraction measurements, (this symposium), 1963.

King, P. B., The evolution of North America, Princeton Univ. Press, 1959.

Mohorovicic, A., Das beben vom 8, 1909, Jahrb. Meteorol. Observatorium Zagreb, 9, Pt. IV, Sect. 1, 63, 1910.

Mota, Lindonor, Determination of dips and depths of geological layers by the seismic refraction method, Geophysics, 19, 242-254, 1954.

Pakiser, L. C., Structure of the crust and upper mantle in the western United States, (this symposium), 1963.

Ryall, Alan, and David J. Stuart, Traveltimes and amplitudes from nuclear explosions: Nevada Test Site to Ordway, Colorado, (this symposium), 1963.

Tocher, Don, Seismic velocities and structure in northern California and Nevada, Ph.D. Thesis, Univ. of California, 1956.

Warrick, R. E., and others, The specification and testing of a seismic-refraction system for crustal studies, Geophysics, 26, 820-824, 1961.